

# Water Resources Research

## RESEARCH ARTICLE

10.1029/2021WR030203

### Key Points:

- A parsimonious snow module is developed based on Budyko's framework to improve an existing physics-based dynamic water balance model
- A monthly parameterization is proposed to reflect the seasonal behavior of catchment characteristics
- The augmented model that includes snow with monthly parameterization shows significant improvements in simulating monthly streamflow

### Correspondence to:

J. Hwang,  
[jh4501@columbia.edu](mailto:jh4501@columbia.edu)

### Citation:

Hwang, J., & Devineni, N. (2022). An improved Zhang's dynamic water balance model using Budyko-based snow representation for better streamflow predictions. *Water Resources Research*, 58, e2021WR030203. <https://doi.org/10.1029/2021WR030203>

Received 13 APR 2021

Accepted 21 DEC 2021

## An Improved Zhang's Dynamic Water Balance Model Using Budyko-Based Snow Representation for Better Streamflow Predictions

Jeongwoo Hwang<sup>1,2</sup>  and Naresh Devineni<sup>2</sup> 

<sup>1</sup>Department of Earth and Environmental Engineering, Columbia University, New York, NY, USA, <sup>2</sup>Department of Civil Engineering, The City University of New York (City College), New York, NY, USA

**Abstract** Understanding the water balance of a catchment in relation to its regional climate forcings and catchment characteristics is critical for predicting current and future water resources amid changing climate and land cover. This study intends to improve Zhang's monthly water balance model (a physics-based conceptual hydrologic model) that reflects the physical partitioning process of the hydrological cycle at the basin level based on regional climate and catchment characteristics. The existing model does not include snow process and has confronted evident limitations in snow-affected areas, which is a critical aspect since snowmelt water has been a significant source of water resources for many regions, especially in the temperate and frigid zones. We introduce a snow module based on surface energy balance and Budyko-limits on melting and combine it with the existing water balance equations. Moreover, monthly parameterization is applied to the model to better explain the time-varying hydrological characteristics of a catchment. The proposed model involves five different monthly parameters, which determine the physical partitioning process of the hydrological cycle, and they are regionally calibrated and validated under Budyko-type constraints. The model is applied to 1,210 basins across the continental United States (CONUS), and the simulated streamflow is compared to the observed data. The proposed model significantly outperformed the original model, improving the median NSE by 31% (from 0.51 to 0.67) and increasing the number of catchments with an acceptable NSE by 58%. The spatial variability of the basin characteristics across the CONUS is also investigated based on the calibrated parameters.

### 1. Introduction

Sufficient understanding of the hydrological processes and catchment controls is essential for predicting water availability and enhancing water resources reliability for human society and ecology. In this regard, several critical studies have shown that the intricate interactions between climatic forcings (precipitation and temperature/potential evapotranspiration) and catchment characteristics are the dominant controls for the water balance of a catchment (Eagleson, 1978; Farmer et al., 2003; Milly, 1994; Zhou et al., 2015). Accordingly, hydroclimatic models are often adopted to simplify the complex hydroclimatological process by selectively amplifying a system's fundamental aspects at the expense of incidental details. Thus, a model is considered ideal when it is simple enough to understand and use while complex enough to reflect the hydrological process (Anderson & Burt, 1985). To this end, numerous hydrological models have been developed along with the advances in hydrology, data collection, and computational capability (Beven et al., 1995; Fekete et al., 2010; Liang et al., 1994; Reggiani et al., 2000; Thomas, 1981; Thornthwaite, 1948; L. Zhang et al., 2008).

An empirical study conducted by Budyko (1961) estimates the long-term water balance by introducing a simple supply-demand relationship between the long-term available surface energy and water. Also known as *Budyko's framework*, this concept has been used to build water balance models. The significance of such water balance models lies in the fact that they generally explain the fundamental aspects of a hydrological process sufficiently with a relatively small number of inputs and model parameters (Koster & Suarez, 1999; Milly, 1994; Sankarasubramanian & Vogel, 2002). As the water demand continues to increase, there has been a growing interest in predicting water availability for ungauged watersheds (Franks et al., 2005; Sivapalan et al., 2003). However, quantifying the impacts of climate variability and land-use/land-cover changes on hydrology and predicting streamflow in these ungauged catchments have remained challenging (Sivapalan et al., 2003; L. Zhang et al., 2004). Subsequently, Budyko-based models have been gaining attention since they have the potential for monthly runoff

predictions or impact assessment of land-use/land-cover changes in ungauged catchments by taking advantage of its parameter parsimony (Sankarasubramanian et al., 2020; L. Zhang et al., 2008).

Budyko-based water balance models at longer timescales (annual to decadal) have shown a good performance (Li et al., 2013; Padrón et al., 2017; Yang et al., 2007) and have been further improved by introducing additional controls, including soil-moisture holding capacity, rainfall seasonality, vegetation characteristics, snow ratio, and human influences (Sankarasubramanian et al., 2020; Sankarasubramanian & Vogel, 2002; L. Zhang et al., 2001; D. Zhang et al., 2015). Extending these Budyko-based water balance models to finer timescales requires the incorporation of additional processes. L. Zhang et al. (2008) argued that rainfall variation, potential evapotranspiration, and water storage must be considered when modeling water balance at sub-annual timescales. In response, they proposed a sub-annual water balance model with a multi-layer structure to comprise storage control and mimic the physical partitioning process. Based on a top-down approach (Sivapalan & Young, 2006), the proposed model extends the "supply-demand" concept of Budyko's framework for two critical partitioning processes—separation of precipitation into catchment retention and direct runoff, and separation of water availability into evapotranspiration, soil moisture storage, and groundwater recharge. The partitioning process of the model is controlled by four efficiency and partitioning parameters in total, and each of these parameters represents a hydrological characteristic of a catchment. This parsimonious physics-based structure of Zhang's dynamic water balance model (ZDWBM) provides an advantage over other hydrologic models that simulate monthly water balance (Mouelhi et al., 2006; Vandewiele & Xu, 1992; Wang et al., 2014; Xiong & Guo, 1999). The *abcd* model, proposed by Thomas (1981), involves a partitioning process comparable to that of the ZDWBM, but the evapotranspiration and baseflow are treated differently. Moreover, the ZDWBM allows both linear and nonlinear relationships (as the process demands) during the partitioning, whereas the *abcd* model only allows nonlinear relationships.

Although several studies have confirmed ZDWBM's capability in predicting monthly runoff for various regions (P. Bai et al., 2015; Tekleab et al., 2011; L. Zhang et al., 2008), the model is found to perform poorly in many watersheds across the continental United States (Petersen et al., 2018). It is especially true for regions where snowmelt plays a significant role—the model performance degrades as catchment elevation and latitude increases (Petersen et al., 2018). Such underperformance in those regions reflects the limitation of the model without snowmelt controls. This limitation could be a critical aspect since snowmelt is often considered a significant water source for many catchments (Barnett et al., 2005; Stewart et al., 2005). Therefore, improvements to the ZDWBM are required to account for snowmelt effects in the hydrological cycle.

Several studies included snow components in Budyko-based models, but they are mostly based on a simple temperature-based model (Deng et al., 2018; Martinez & Gupta, 2010), degree-day method (J. Bai et al., 2018), or for long-term scales (D. Zhang et al., 2015). These methods require multiple additional parameters, may be insufficient to represent the actual snow melting, or excessively increase the model's complexity. Here, we first explore the limitations of ZDWBM in modeling monthly water balance based on more than 1,200 unmodified basins across the continental United States and propose a novel snow module for improving the model, extending the supply-demand concept of Budyko's framework based on the surface energy balance. The proposed snow module introduces only one additional parameter, minimizing the increase in model complexity. The augmented model with snow module is also tested with monthly parameters to represent the seasonal variability of catchment characteristics better.

## 2. Data Description

For this study, we only focus on unmodified basins and thus employ a hydroclimatological dataset developed by Vogel and Sankarasubramanian (2005), which contains lumped-average monthly precipitation, temperature, and potential evapotranspiration of the continental United States (CONUS) catchments. The dataset was developed for catchments where monthly streamflow measurements are also available from the Hydroclimatic Data Network (HCDN) database, developed by Slack et al. (1993). HCDN catchments are found to be minimally affected by human influences, which makes them specifically suitable for exploring surface-water conditions under fluctuations in prevailing climatic conditions (Slack et al., 1993). A detailed description of the HCDN data set can be found in Vogel et al. (1999), Vogel and Sankarasubramanian (2000), and Sankarasubramanian and Vogel (2002). We focus on HCDN basins across the CONUS, and they are classified into three groups: snow-dominated basins, snow-affected basins, and basins least affected by snow (Figure 1). The classification is based on a snow-factor

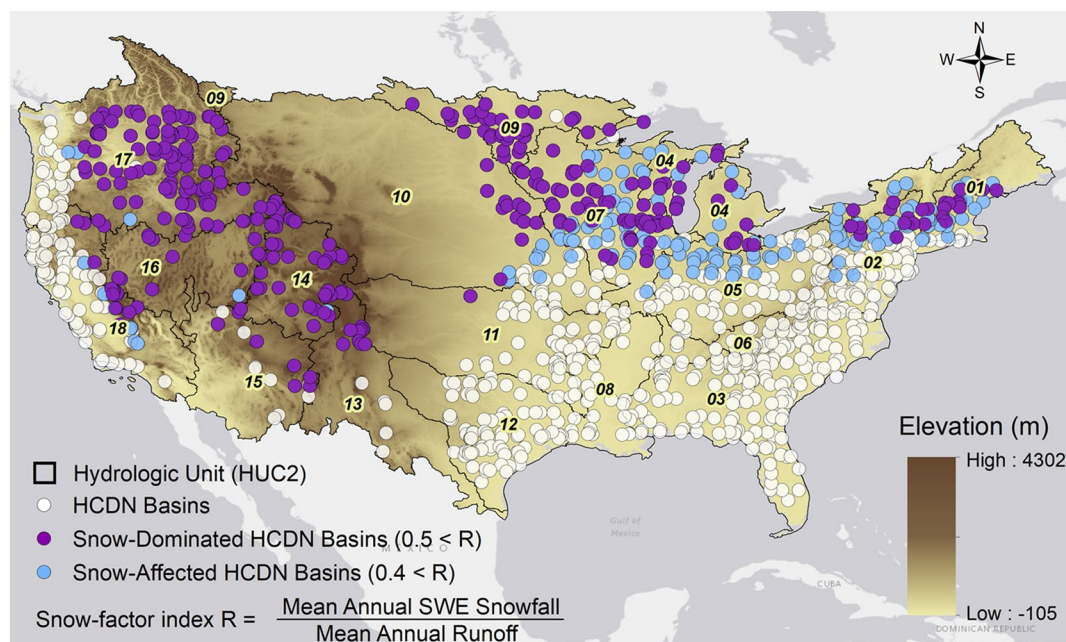


**Figure 1.** Spatial distribution of the selected HCDN basins across the continental United States.

index ( $R$ ) which measures the proportion of snow to streamflow in a catchment (Barnett et al., 2005). Here we calculated  $R$  as a unitless index by dividing the mean annual snow-water equivalent (SWE) of snowfall [ $L$ ] (i.e., the amount of water substance contained within snowfall) by the area normalized mean annual streamflow [ $L$ ]. The procedure of determining SWE of snowfall is presented in Section 3.2. One may define snow basins by calculating the ratio of SWE to precipitation instead of streamflow, as it may better represent the control of snow on the water budget of the basin. However, as this study focuses on improving an existing runoff model, especially for snow affected basins, we insist on calculating  $R$  based on streamflow since it may better represent areas where the existing model may perform poorly. The annual-basis calculation of  $R$  is assumed to represent the long-term contribution of snow to runoff. Based on this calculation, most of the catchments in CONUS show  $R$  values between 0 and 1. Catchments with  $R > 0.4$  are classified as “snow-affected,” and those with  $R > 0.5$  are categorized as “snow-dominated.” Based on this measure, 41% of the selected HCDN basins are at least snow-affected, and more than 28% are snow-dominated. The snow-factor index is computed based on the precipitation data, following the procedure presented in Section 3.3.

### 2.1. Streamflow Data

The HCDN database contains daily mean streamflow for 1,659 HCDN basins across the United States. It is subjected to six different criteria for quality assurance by the United States Geological Survey (USGS): (1) Availability of data in electronic form—data is available in electronic format; (2) Breadth of coverage—records from any station for any water year through 1988 are considered; (3) Length of record—record lengths are at least 20 years unless the record is available for a uniquely located surface-water gauging station; (4) Accuracy of the records—accuracy ratings of records are at least “good” as defined by USGS standards, which could be found in the USGS Water-Data Reports for each State, published annually, as well as in the report by Rantz (1982); (5) Unimpaired basin conditions—there is no overt adjustment of “natural” monthly streamflows by any form of regulations; (6) Measured discharge values—only measured discharge values are tabulated, whereas reconstructed or estimated records are not used. Streamflow records vary by catchment, ranging from 1874 to 1988, with an average record length of  $\sim 44$  years. For this study, we only considered basins with continuous streamflow data for at least 10 years between 1957 and 1988, and this criterion yielded 1,210 HCDN basins for further investigation. The average record length of the selected sites is approximately 31 years.

## 2.2. Climate Forcings Data

Vogel and Sankarasubramanian (2005) compiled a monthly climate dataset containing lumped average monthly minimum and maximum temperature, precipitation, and potential evapotranspiration for 1,376 HCDN watersheds. The lumped average temperature and precipitation data were derived by using the Precipitation Elevation Regression on Independent Slopes Model (PRISM) climate analysis system (Daly et al., 1994). PRISM distributes point measurements to evenly spaced 2.5 min (~4 km) grids while accounting for orographic effects and other elevation-related effects. It should be noted that the HCDN precipitation data includes both rainfall and snow water equivalent without any distinction. Monthly potential evapotranspiration data were computed using the Hargreaves method (Hargreaves & Samani, 1982). The Hargreaves method estimates  $PET$  based on an empirical equation that is a function of air temperature and extraterrestrial radiation. Extraterrestrial solar radiation was estimated for each HCDN basin by computing the solar radiation over  $0.1^\circ$  grids using the method introduced by Duffie and Beckman (1980) and then summing those estimates over the entire basin (Sankarasubramanian & Vogel, 2002). The Hargreaves method was the highest ranked temperature-based method for computing potential evapotranspiration reported in American Society of Civil Engineers (ASCE) Manual 70 analysis (Jensen et al., 1990).

## 3. Methods

### 3.1. Zhang's Dynamic Water Balance Model (ZDWBM)

Budyko (1961) has inferred a functional relationship between atmospheric demand, water supply, and water balance for longer time scales, assuming the water storage component is negligible under a steady state. This idea can be applied to unmodified catchments by considering precipitation ( $P$ ) as the water available, and potential evapotranspiration ( $PET$ ) as the atmospheric demand. Under dry conditions, where  $PET$  is significantly greater than  $P$ , the actual evapotranspiration ( $ET$ ) is limited by  $P$ . During wet periods, meanwhile,  $PET$  is extremely less than  $P$ . Thus,  $ET$  would be limited by  $PET$ . This supply-demand limit concept of Budyko's framework can be expressed as

$$ET = f(P, PET)$$

$$\text{When } \frac{PET}{P} > 1 (\text{dry conditions}), ET \rightarrow P \text{ as } \frac{PET}{P} \rightarrow \infty$$

$$\text{When } \frac{PET}{P} < 1 (\text{wet conditions}), ET \rightarrow PET \text{ as } \frac{PET}{P} \rightarrow 0$$

Budyko's framework is recognized as a Darwinian approach because of this empirical nature of understanding the overall hydrological process from observations and a constitutive equation (Harman & Troch, 2014; Wang et al., 2016). Due to its simplicity, several studies have attempted to develop a water balance model based on this framework (Chen et al., 2013; Greve et al., 2015; D. Wang & Tang, 2014; L. Zhang et al., 2008) and tested various mathematical equations (Budyko et al., 1974; Fu, 1981; Pike, 1964; Schreiber, 1904; L. Zhang et al., 2001) that comply with this concept. Fu (1981) has proposed an equation ( $F$ ) through mathematical reasoning to describe this functional relationship between mean annual  $P$ ,  $ET$ , and  $PET$  as

$$\frac{\overline{ET}}{\overline{P}} = F\left(\frac{\overline{PET}}{\overline{P}}, \alpha\right) = 1 + \frac{\overline{PET}}{\overline{P}} - \left[1 + \left(\frac{\overline{PET}}{\overline{P}}\right)^{\frac{1}{1-\alpha}}\right]^{1-\alpha} \quad (1)$$

where  $\overline{P}$ ,  $\overline{PET}$ , and  $\overline{ET}$  are mean annual precipitation, potential evapotranspiration, and evapotranspiration, respectively, while  $\alpha$  is the model parameter that ranges from 0 to 1. Arguing that Fu's equation outperforms other similar equations in estimating mean annual evapotranspiration (L. Zhang et al., 2004), L. Zhang et al. (2008) have incorporated this equation into Budyko's framework to develop a water balance model that could reflect the physical partitioning process. This combination of Darwinian approach and physical partitioning process enables Zhang's dynamic water balance model (ZDWBM) to achieve parameter parsimony, making the model suitable for ungauged catchments.

As the water balance of a catchment becomes highly sensitive to changes in storage at finer timescales, ZDWBM takes storage controls into account to make itself suitable for sub-annual time scales. The storage controls consist

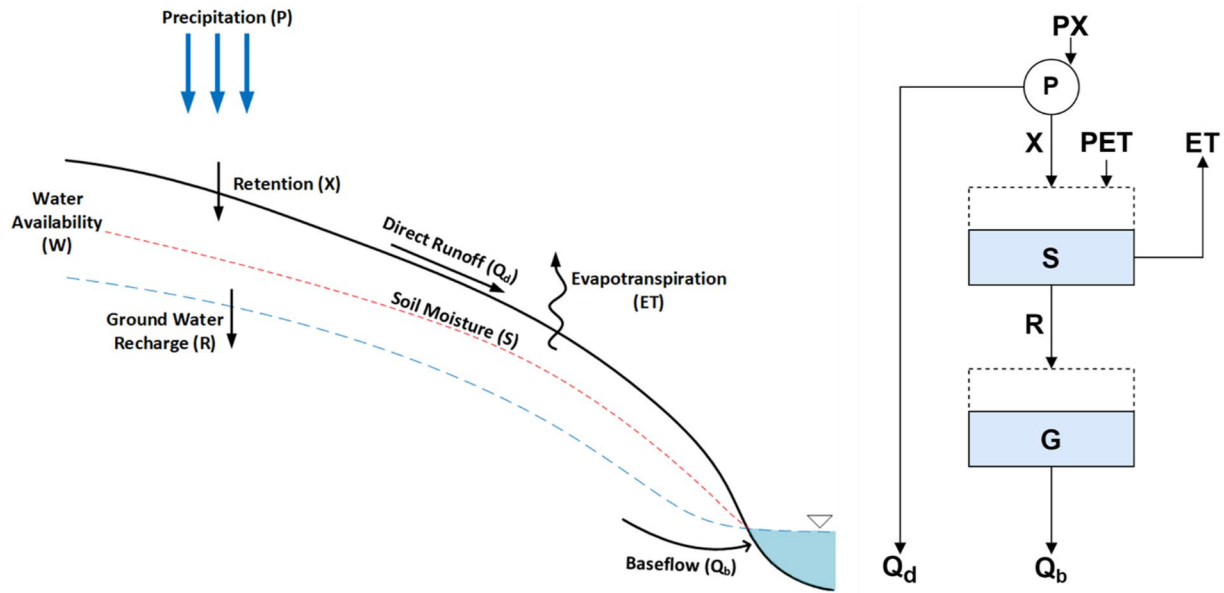


**Figure 2.** Diagram of the hydrological partitioning process of the ZDWBM (left) and the corresponding flowchart (right).

of two different water volumes—soil-moisture storage and groundwater storage. The soil-moisture storage is the water in the vadose zone sensitive to the atmospheric demand and likely to evaporate or transpire. In contrast, groundwater storage is mainly controlled by the soil-moisture dynamics. Besides, ZDWBM generalizes the method of Budyko (1961) estimating  $ET$  with a supply-demand framework to model other water balance components, which will be shown during this section. A diagram that illustrates the partitioning process and major hydrological components of ZDWBM is presented in Figure 2 with a simplified flowchart alongside. ZDWBM mathematically describes the hydrological cycle by starting from partitioning precipitation ( $P_t$ ) into direct runoff ( $Q_t^d$ ) and catchment retention ( $X_t$ ) for any given timestep  $t$  as

$$P_t = Q_t^d + X_t \quad (2)$$

where  $X_t$  is defined as catchment rainfall retention, which is the amount of rainfall retained by the catchment for evapotranspiration ( $ET_t$ ), change in soil-moisture storage ( $S_t - S_{t-1}$ ), and groundwater recharge ( $R_t$ ). This  $X_t$  can be modeled with the supply-demand limit concept by presuming its atmospheric demand limit ( $PX_t$ ) as the sum of potential evapotranspiration ( $PET_t$ ) and available storage capacity of soil water ( $S_{max} - S_{t-1}$ ), where  $S_{max}$  is a model parameter that indicates the maximum soil-moisture storage capacity. The water availability limit of  $X_t$  is approximated as  $P_t$ . Based on Budyko's framework, therefore, L. Zhang et al. (2008) postulate the relationship between  $X_t$ ,  $PX_t$ , and  $P_t$  as

$$\text{When } \frac{PX_t}{P_t} > 1 (\text{dry conditions}), X_t \rightarrow P_t \text{ as } \frac{PX_t}{P_t} \rightarrow \infty$$

$$\text{When } \frac{PX_t}{P_t} < 1 (\text{wet conditions}), X_t \rightarrow PX_t \text{ as } \frac{PX_t}{P_t} \rightarrow 0$$

and employs Fu's equation to estimate the actual catchment rainfall retention  $X_t$ :

$$\frac{X_t}{P_t} = F \left( \frac{PX_t}{P_t}, \alpha_1 \right) \quad (3)$$

$$X_t = P_t \left[ 1 + \frac{PX_t}{P_t} - \left\{ 1 + \left( \frac{PX_t}{P_t} \right)^{\frac{1}{1-\alpha_1}} \right\}^{1-\alpha_1} \right] \quad (4)$$

$$X_t = P_t \left[ 1 + \frac{PET_t + (S_{max} - S_{t-1})}{P_t} - \left\{ 1 + \left( \frac{PET_t + (S_{max} - S_{t-1})}{P_t} \right)^{\frac{1}{1-\alpha_1}} \right\}^{1-\alpha_1} \right] \quad (5)$$

where  $\alpha_1$  is defined as retention efficiency that ranges from 0 to 1. The larger  $\alpha_1$  is, the more retention and less direct runoff are expected.

Then, water availability of a catchment ( $W_t$ ) can be estimated following its definition, the combination of  $X_t$  and  $S_{t-1}$ :

$$W_t = X_t + S_{t-1} \quad (6)$$

Considering the aforementioned definition of  $X_t$ , Equation 6 could be rewritten as

$$W_t = ET_t + S_t + R_t \quad (7)$$

The sum of  $ET_t$  and  $S_t$  is referred to as evapotranspiration opportunity ( $Y_t$ ), the potential amount of water that can evaporate or transpire from the vadose zone (Sankarasubramanian & Vogel, 2002). The atmospheric demand limit of  $Y_t$  is approximated as the sum of  $S_{max}$  and  $PET_t$ , while the water supply limit is the available water  $W_t$ . Based on the supply-demand limit concept, L. Zhang et al. (2008) formulated the evapotranspiration opportunity of a catchment,  $Y_t$ , with Fu's equation as

$$\frac{Y_t}{W_t} = F \left( \frac{S_{max} + PET_t}{W_t}, \alpha_2 \right) \quad (8)$$

$$Y_t = W_t \left[ 1 + \frac{S_{max} + PET_t}{W_t} - \left\{ 1 + \left( \frac{S_{max} + PET_t}{W_t} \right)^{\frac{1}{1-\alpha_2}} \right\}^{1-\alpha_2} \right] \quad (9)$$

where  $\alpha_2$  is a model parameter defined as the evapotranspiration efficiency that ranges from 0 to 1.

Meanwhile, the evapotranspiration component  $ET_t$  is assumed to have an atmospheric limit of potential evapotranspiration ( $PET_t$ ) and a water supply limit of catchment water availability ( $W_t$ ). Rooted in Budyko's framework and Fu's equation, therefore,  $ET_t$  is obtained by

$$\frac{ET_t}{W_t} = F \left( \frac{PET_t}{W_t}, \alpha_2 \right) \quad (10)$$

$$ET_t = W_t \left[ 1 + \frac{PET_t}{W_t} - \left\{ 1 + \left( \frac{PET_t}{W_t} \right)^{\frac{1}{1-\alpha_2}} \right\}^{1-\alpha_2} \right] \quad (11)$$

where  $\alpha_2$  is the same model parameter from Equation 8. By obtaining  $Y_t$  and  $ET_t$ , groundwater recharge  $R_t$  can now be estimated by rewriting Equation 7 as

$$R_t = W_t - Y_t \quad (12)$$

It should be noted that the parameter sharing between Equations 8 and 10 ensures that groundwater recharge  $R_t$  is essentially governed by evapotranspiration efficiency  $\alpha_2$ . That is, larger (smaller) values of  $\alpha_2$  results in less (more) groundwater recharge  $R_t$  in the catchment.

Considering the definition of  $Y_t$ , soil-moisture storage ( $S_t$ ) can be now determined as:

$$S_t = Y_t - ET_t \quad (13)$$

ZDWBM assumes groundwater storage ( $G_t$ ) as a linear reservoir, and thus, groundwater balance is estimated as

$$G_t = (1 - d)G_{t-1} + R_t \quad (14)$$

$$Q_t^b = d(G_{t-1}) \quad (15)$$

where  $Q_t^b$  is baseflow, and  $d$  is a model parameter which represents the proportion of groundwater transferred to the baseflow for each given timestep  $t$ . Finally, the total streamflow ( $Q_t$ ) can be obtained by the summation of direct runoff  $Q_t^d$  and the base flow  $Q_t^b$  as written as follows:

$$Q_t = Q_t^d + Q_t^b \quad (16)$$

To summarize, ZDWBM estimates catchment scale sub-annual runoff with climate forcings such as  $P_t$  and  $PET_t$  based on four different model parameters—retention efficiency ( $\alpha_1$ ), evapotranspiration efficiency ( $\alpha_2$ ), groundwater coefficient ( $d$ ), and maximum soil-moisture storage capacity ( $S_{max}$ ). These parameters are calibrated based on four objective functions which determine the dissimilarity between estimated and observed runoff data for each tested catchment. Each of these objective functions places different weights on errors in low flows, high flows, time shift between estimated and observed, and mass balance over the period of calibration. A set of parameter values that minimizes the mean of those four objective functions are assumed to represent the regional characteristics of the climate and basin.

### 3.2. Implantation of a Budyko-Based Snow Module to ZDWBM

The idea of Budyko's framework stems from the concept of long-term energy and water balance, which both are subjected to the principle of conservation, assuming the ground heat and subsurface water storage components are negligible. The long-term energy and water balance of a catchment can be mathematically expressed, respectively, as

$$Rn = L_E \cdot ET + Hn \quad (17)$$

$$P = ET + Q \quad (18)$$

where  $Rn [M/T^2]$  is the net radiative heat flux from the atmosphere to land surface,  $L_E [M/L \cdot T^2]$  is the latent heat of evaporation,  $ET [L]$  is evapotranspiration,  $Hn [M/T^2]$  is the sensible heat, the heat transfer from land surface to atmosphere,  $P [L]$  is precipitation, and  $Q [L]$  is runoff. The division of Equation 17 by the latent heat of evaporation ( $L_E$ ) yields an energy-balance constraint on evapotranspiration ( $ET$ ):

$$\frac{Rn}{L_E} = ET + \frac{Hn}{L_E} \quad (19)$$

The above equation implies that the maximum possible  $ET$  occurs when the sensible heat is negligible, and the incoming radiative energy is exclusively consumed by  $ET$  while the amount of water available for  $ET$  is unlimited in the subsurface. This maximum possible evapotranspiration is thus numerically equivalent to  $Rn/L_E$  and is conceptually referred to as potential evapotranspiration ( $PET$ ) (Budyko et al., 1974; Sposito, 2017; D. Zhang et al., 2015). As the Hargreaves method estimates  $PET$  based on an empirical equation that is a function of air temperature and extraterrestrial radiation, parameterizing  $PET$  in the snow model by surface radiation ( $Rn$ ) and specific latent heat ( $L_E$ ) is assumed to have a reasonable connection to the concept of  $PET$  from the Hargreaves method. In this regard, we expect there would be minimum or no loss of information from this approximation.

Since  $ET$  simultaneously acts as the primary process for both long-term water balance and energy balance as shown in Equations 18 and 19, it is possible to conclude that a functional relationship between water and energy balance exists:

$$\frac{ET}{P} = f\left(\frac{PET}{P}\right) \quad (20)$$

which is referred to as Budyko's framework as mentioned in the previous subsection.

To improve the existing dynamic water balance model proposed by L. Zhang et al. (2008), especially in snow-affected regions, we developed a snow module that could be implanted into the model. The proposed snow module takes the effect of snow into account and follows the logic of Budyko's framework as well to preserve the spirit of, and parameter parsimony that is achieved from ZDWBM. The snow and water balance for any monthly timestep  $t$  are jointly considered as

$$SF_t + SP_{t-1} = M_t + SP_t \quad (21)$$

$$M_t + RF_t = ET_t + Q_t + \Delta S_t \quad (22)$$

where  $SF_t [L]$  is the snow-water equivalent (SWE) of snowfall,  $SP_t [L]$  is the SWE of snowpack,  $M_t [L]$  is the snowmelt,  $RF_t [L]$  is rainfall, and  $\Delta S_t [L]$  is the change in soil-moisture storage. Equation 21 indicates that the given amount of snow is equivalent to the sum of snowmelt and the remaining snowpack, neglecting snow sublimation and deposition. We discuss the implications of this assumption in Section 5.2.

Since precipitation from the HCDN database provides the sum of rainfall and SWE of snowfall without any distinction, each amount of rainfall and snowfall must be determined. Here  $P_t$  is partitioned into  $RF_t$  and  $SF_t$  based on the monthly average of daily min and max temperatures ( $T_t^{avg}$ ):

$$\text{If } T_t^{avg} \leq -0.5^\circ\text{C, then } RF_t = 0 \text{ and } SF_t = P_t$$

$$\text{If } T_t^{avg} \geq +0.5^\circ\text{C, then } RF_t = P_t \text{ and } SF_t = 0$$

$$\text{Else, } RF_t = P_t(0.5^\circ\text{C} + T_t^{avg}) \text{ and } SF_t = P_t(0.5^\circ\text{C} - T_t^{avg})$$

Here the threshold temperatures for the partitioning of precipitation were determined as  $-0.5$  and  $0.5^\circ\text{C}$ , and the partitioning scheme assumes a linear relationship in phase changes between snowfall and rainfall (Andreadis et al., 2009; Hamlet et al., 2005; H. Wu et al., 2014). Also, our snow module assumes the ground freezes during snow accumulating phases. Land surface energy and water balance can be greatly affected by the seasonal freeze and thaw cycles of the ground. Seasonal freezing of the ground occurs widely across the world to such an extent that up to nearly 50% of the exposed lands in the Northern Hemisphere may experience seasonal freezing (T. Zhang et al., 2003). To reflect such aspect in our model, we assume the initial subsurface water storage  $S_{t-1}$  freezes and becomes a part of the snow contents when the mean temperature ( $T_t^{avg}$ ) is less than  $-0.5^\circ\text{C}$  at timestep  $t$ . In this case, Equation 21 can be rewritten as

$$SF_t + SP_{t-1} + S_{t-1} = M_t + SP_t \quad (23)$$

and  $S_{t-1}$  (water) becomes 0.

Since the process of melting consumes energy, as does evapotranspiration, the intra-annual energy balance equation can be expressed in a similar form to Equation 17 as,

$$Rn_t = L_E \cdot ET_t + L_F \cdot M_t + Hn_t + G_t \quad (24)$$

where  $L_F [M/L \cdot T^2]$  is the latent heat of fusion, and  $G_t [M/T^2]$  is the ground heat flux. As both the processes of snow melting and evapotranspiration simultaneously absorb energy, especially during melting seasons, while the given amount of  $Rn_t$  is limited, the maximum possible energy for each phase transition is determined as a fraction of the incoming  $Rn_t$ , assuming  $Hn_t$  and  $G_t$  are fully occupied for the phase transitions. Previous energy balance studies in different locations argue that net radiation contributes most of the energy available for melting (Boudhar et al., 2016; Fayad et al., 2017; Mazurkiewicz et al., 2008).

When a substantial amount of energy is supplied to a surface containing snow, both evaporation and melting start absorbing energy competitively (Miller, 1982). An exact division of the total energy available for the phase change processes of evaporation and melting is challenging since it involves complex heat and mass transfer processes of a system with large temporal and spatial variations. An experimental study conducted by Shook and Gray (1997) argued that more than 90% of the total energy available for phase changes is allocated for melting rather than evaporation in open environments with continuous snowpacks. At a basin scale, however, snowpacks are rarely continuous in monthly timescale. Thus, it might be inappropriate to consider this estimate as the absolute fraction for partitioning the total energy for  $ET_t$  and  $M_t$ . Instead, we assume net  $Rn_t$  is partitioned for  $ET_t$  and  $M_t$  based on the mass ratio of water and snow contents in the catchment, respectively:

$$Rn_t = Re_t + Rm_t \quad (25)$$

$$Re_t = \left( \frac{RF_t + S_{t-1}}{SF_t + SP_{t-1} + RF_t + S_{t-1}} \right) \cdot Rn_t \quad (26)$$

$$Rm_t = \left( \frac{SF_t + SP_{t-1}}{SF_t + SP_{t-1} + RF_t + S_{t-1}} \right) \cdot Rn_t \quad (27)$$

where  $Re_t$  [ $M/T^2$ ] and  $Rm_t$  [ $M/T^2$ ] are the maximum possible energies distributed for  $ET_t$  and  $M_t$ , respectively. This setup yields an energy fraction similar to that from Shook and Gray (1997) for extreme snow-dominating situations. This calculation method can be considered conceptually reasonable for obtaining a rough estimate of the energy partition for any generalized case. For example, the proportion of total energy for  $ET_t$  is expected to increase when snowpacks become patchy and accompanied by increased air temperature (higher saturation vapor pressure) and snowmelt water. Meanwhile, when the snowpack accumulates in the presence of low air temperature, the total given amount of energy for phase transitions may be small. However, the proportion of the total energy for  $M_t$  is likely to increase due to the low air temperature (lower saturation vapor pressure), increased snow component, and water loss by freezing. That is, the ratio of the available energy between  $ET_t$  and  $M_t$  can be roughly estimated in proportion to the mass ratio of water and snow. Further, as this water/snow partitioning is based on temperature and precipitation, the temporal continuity of snowpack follows that of the temperature and precipitation profiles. Snowpack is determined at a catchment scale and assumed to be homogenous within the catchment, as the model in this study is a catchment lumped model where precipitation and temperature are also aggregated in a catchment scale. That is, we assume a spatial homogeneity in the fluxes of snowpack across each basin.

Then, the maximum possible evapotranspiration and melting are computed with the given  $PET_t$  dataset since it can derive the net total available energy for phase transitions:

$$\begin{aligned} PET_t^* &= \frac{Re_t}{L_E} = \left( \frac{RF_t + S_{t-1}}{SF_t + SP_{t-1} + RF_t + S_{t-1}} \right) \cdot \frac{Rn_t}{L_E} \\ &= \left( \frac{RF_t + S_{t-1}}{SF_t + SP_{t-1} + RF_t + S_{t-1}} \right) \cdot PET_t \end{aligned} \quad (28)$$

$$\begin{aligned} PM_t &= \frac{Rm_t}{L_F} = \left( \frac{SF_t + SP_{t-1}}{SF_t + SP_{t-1} + RF_t + S_{t-1}} \right) \cdot \frac{Rn_t}{L_F} \\ &= \left( \frac{SF_t + SP_{t-1}}{SF_t + SP_{t-1} + RF_t + S_{t-1}} \right) \cdot \frac{Rn_t}{(0.15 \cdot L_E)} \\ &= \left( \frac{SF_t + SP_{t-1}}{SF_t + SP_{t-1} + RF_t + S_{t-1}} \right) \cdot \left( \frac{1}{0.15} \right) \cdot PET_t \end{aligned} \quad (29)$$

where  $PET_t^*$  [ $L$ ] is the newly computed potential evapotranspiration and  $PM_t$  [ $L$ ] is *potential melting*, which is the maximum possible melting. Here, we compute  $PET_t^*$  with the existing  $PET_t$ , which is the potential amount of evapotranspiration when the radiative energy is monopolized only by the evapotranspiration process. As the specific latent heat of fusion ( $334 \text{ kJ/kg}$ ) is  $\sim 0.15$  times the specific latent heat of evaporation ( $2265 \text{ kJ/kg}$ ),  $PM_t$  is obtained with the existing  $PET_t$  using this ratio.

Now  $M_t$  could be obtained by establishing a functional relationship based on the logic of Budyko's framework, approximating the supply limit of  $M_t$  as given amount of snow ( $SF_t + SP_{t-1}$ ), and the atmospheric demand limit as  $PM_t$ . This could be mathematically expressed using Fu's equation as

$$\frac{M_t}{SF_t + SP_{t-1}} = F \left( \frac{PM_t}{SF_t + SP_{t-1}}, \beta \right) \quad (30)$$

$$M_t = (SF_t + SP_{t-1}) \left[ 1 + \frac{PM_t}{SF_t + SP_{t-1}} - \left[ 1 + \left( \frac{PM_t}{SF_t + SP_{t-1}} \right)^{\frac{1}{1-\beta}} \right]^{1-\beta} \right] \quad (31)$$

where  $\beta$  is a parameter that indicates the melting efficiency of a catchment, ranging from 0 to 1, that is, a larger  $\beta$  will result in more snow melting. When there is no snow content in the given catchment, it is obvious there should be no snow melting either. The absence of snow contents at timestep  $t$  mathematically leads the  $(SF_t + SP_{t-1})$  element on the right-hand side of Equation 31 to be 0, and thus  $M_t$  always converge to 0 as well, regardless of the value of  $\beta$ . Because of this aspect, the calibration process of the model assigns an arbitrary value to  $\beta$ , misrepresenting the catchment's melting efficiency when snow contents do not exist in a catchment. In order to overcome such a problem, the calibrated  $\beta$  for catchments with mean annual snow less than 0.1 mm is adjusted as 1 to comply with its concept.

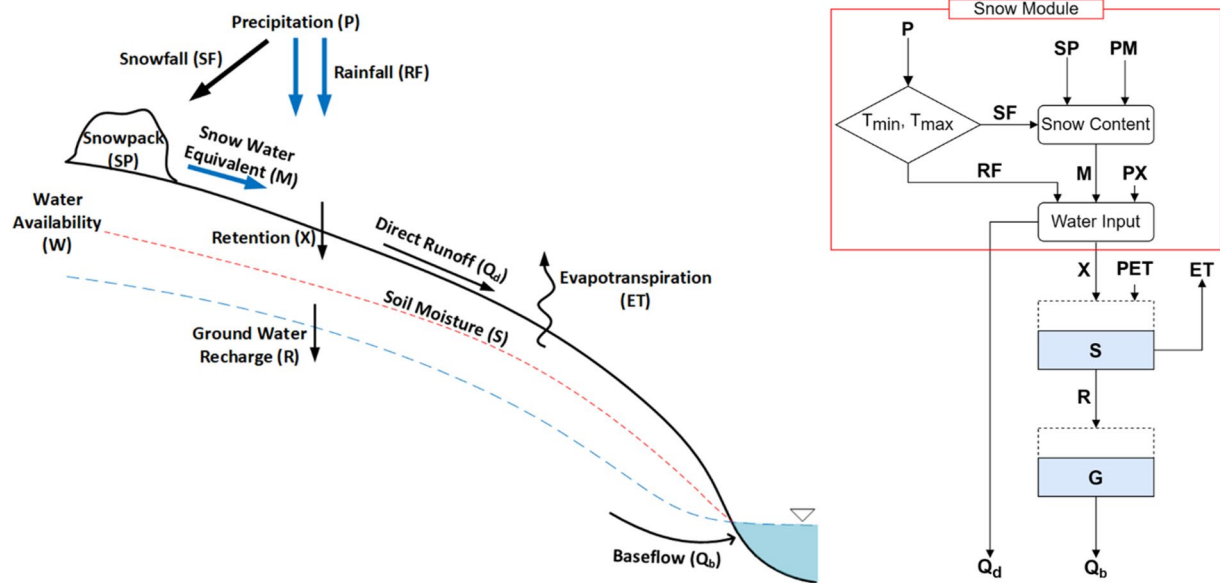


Figure 3. Diagram of the hydrological partitioning process of the snow augmented ZDWB (left) and the corresponding flowchart (right).

Since the proposed snow module defines the input source of water as a combination of rainfall ( $RF_t$ ) and snow-melt ( $M_t$ ), the initial partitioning process of ZDWB is reconstructed as:

$$RF_t + M_t = Q_t^d + X_t \quad (32)$$

The remaining procedure from here is the same as in the original model, as shown in Figure 3.

### 3.3. Monthly Parameterization

The existing ZDWB yields four time-invariant model parameters, each representing different hydrological aspects of the catchment. However, catchment's hydrological responses are often modulated by various factors that manifest in sub-annual time scales, such as antecedent soil moisture, seasonal vegetation, and temperature fluctuations. Thus, while those single-value parameters may partially explain the long-term characteristics of catchments, they might be insufficient to reflect catchments' dynamic response. Moreover, since both snow melting and accumulation processes are extremely season-sensitive, the necessity of developing a time-variant parameterization arises as we intend to include the snow factor in the model. To capture the time-variant catchment properties while minimizing the increase in model complexity at the same time, we set each model parameter to have 12 monthly values. The monthly parameters are optimized by minimizing the dissimilarity between the simulated and observed flows during the calibration period. For each monthly timestep, the model is designed to calibrate the parameter values of the corresponding month. The full model with snow module and monthly parameterization is mathematically presented below:

$$\frac{M_t}{SF_t + SP_{t-1}} = F \left( \frac{PM_t}{SF_t + SP_{t-1}}, \beta_n \right), \text{ where } n = 1 : 12$$

$$\frac{M_t}{SF_t + SP_{t-1}} = 1 + \frac{PM_t}{SF_t + SP_{t-1}} - \left[ 1 + \left( \frac{PM_t}{SF_t + SP_{t-1}} \right)^{\frac{1}{1-\beta_n}} \right]^{1-\beta_n} \quad (32)$$

$$RF_t + M_t = Q_t^d + X_t \quad (33)$$

$$\frac{X_t}{P_t} = F \left( \frac{PX_t}{P_t}, \alpha_{1n} \right), \text{ where } n = 1 : 12 \text{ (months)}$$

$$X_t = P_t \left[ 1 + \frac{PET_t^* + (S_{maxn} - S_{t-1})}{P_t} - \left\{ 1 + \left( \frac{PET_t^* + (S_{maxn} - S_{t-1})}{P_t} \right)^{\frac{1}{1-\alpha_{1n}}} \right\}^{1-\alpha_{1n}} \right] \quad (34)$$

$$W_t = X_t + S_{t-1} \quad (35)$$

$$\frac{Y_t}{W_t} = F \left( \frac{S_{maxn} + PET_t^*}{W_t}, \alpha_{2n} \right), \text{ where } n = 1 : 12 \text{ (months)}$$

$$Y_t = W_t \left[ 1 + \frac{S_{maxn} + PET_t^*}{W_t} - \left\{ 1 + \left( \frac{S_{maxn} + PET_t^*}{W_t} \right)^{\frac{1}{1-\alpha_{2n}}} \right\}^{1-\alpha_{2n}} \right] \quad (36)$$

$$\frac{ET_t}{W_t} = F \left( \frac{PET_t^*}{W_t}, \alpha_{2n} \right), \text{ where } n = 1 : 12 \text{ (months)}$$

$$ET_t = W_t \left[ 1 + \frac{PET_t^*}{W_t} - \left\{ 1 + \left( \frac{PET_t^*}{W_t} \right)^{\frac{1}{1-\alpha_{2n}}} \right\}^{1-\alpha_{2n}} \right] \quad (37)$$

$$R_t = W_t - Y_t \quad (38)$$

$$S_t = Y_t - ET_t \quad (39)$$

$$G_t = (1 - d_n)G_{t-1} + R_t, \text{ where } n = 1 : 12 \text{ (months)} \quad (40)$$

$$Q_t^b = d(G_{t-1}) \quad (41)$$

$$Q_t = Q_t^d + Q_t^b \quad (42)$$

For parameter estimation, an optimization function is solved for each station by minimizing the average of four error functions:

$$\text{Min}(Z), \text{ while } Z = \frac{\sum_{i=1}^4 Z_i}{4} \quad (43)$$

$$Z_1 = \frac{\sum_{i=1}^N [\ln(Q_i^{sim}) - \ln(Q_i^{obs})]^2}{\sum_{i=1}^N [\ln(Q_i^{obs}) - \ln(\overline{Q^{obs}})]^2} \quad (44)$$

$$Z_2 = \frac{\sum_{i=1}^N (Q_i^{sim} - Q_i^{obs})^2}{\sum_{i=1}^N (Q_i^{obs} - \overline{Q^{obs}})^2} \quad (45)$$

$$Z_3 = \frac{\sum_{i=1}^N (Q_i^{sim} - \overline{Q^{sim}})(Q_i^{obs} - \overline{Q^{obs}})}{\sqrt{\sum_{i=1}^N (Q_i^{sim} - \overline{Q^{sim}})^2 \sum_{i=1}^N (Q_i^{obs} - \overline{Q^{obs}})^2}} \quad (46)$$

$$Z_4 = \left\| \ln \left( \frac{\sum_{i=1}^N Q_i^{sim}}{\sum_{i=1}^N Q_i^{obs}} \right) \right\| \quad (47)$$

while,

$$0 \leq \beta_n \leq 1, 0 \leq \alpha_{1n} \leq 1, 0 \leq \alpha_{2n} \leq 1, 0 \leq d_n \leq 1, 0 \leq S_{maxn}$$

where  $Q_i^{sim}$  is the simulated streamflow at time  $i$ ,  $\overline{Q^{sim}}$  is the mean simulated streamflow,  $Q_i^{obs}$  is the observed streamflow at time  $i$ ,  $\overline{Q^{obs}}$  is the mean observed streamflow,  $N$  is the number of timesteps in the calibration period. A set of parameter values that minimizes the mean of those four objective functions is obtained by using

the constrained nonlinear multivariate function (TheMathWorksInc, 2016). For each station, the models run one full-cycle of spin-up over the entire given period with the storage components (soil-moisture, snow, groundwater) at their initial conditions for a stable initialization before calibration ( $S_0 = 0$ ,  $G_0 = 0$ ,  $SP_0 = 0$ ). The estimated storage components from the last timestep of the spin-up are employed as the initial condition for the storages during the calibration process. The observed data was divided into two roughly even parts for each station, and the first 50% of the given observed data were used for calibration, and the later 50% for validation. This is consistent with the calibration and validation process of the original ZDWBM (L. Zhang et al., 2008).

### 3.4. Model Performance Evaluation

For the evaluation of the model, the classic Nash-Sutcliffe efficiency (NSE) coefficient (Nash & Sutcliffe, 1970) between the simulated and observed monthly streamflow were examined ( $NSE = 1 - MSE/\sigma_o^2$  where  $MSE$  is the mean squared error between the simulated and observed monthly flows and  $\sigma_o^2$  is the variance of observed monthly flows). NSE theoretically ranges between  $-\infty$  and 1. Values close to 1 imply that the model can resemble the observed system, whereas values close to 0 mean that the model performance is no better than the mean of the observed. Thus, NSE values less than zero are undesirable. Despite its inherent limitations (Ehret & Zehe, 2011; Gupta & Kling, 2011; Schaeffli & Gupta, 2007), the NSE statistic is one of the evaluation metrics most commonly used for evaluating hydrological model performances. Threshold values of NSE representing a reasonable model performance often depend on the purpose of the model, but a hydrological model at a monthly timestep could be judged *good* when its NSE is greater than 0.65, *satisfactory* when it is greater than 0.5, and *unsatisfactory* if it is less than or equal to 0.5 (Moriassi et al., 2007). We used these threshold values for evaluating our models.

## 4. Results

Here we present the incremental changes in model performance that were observed after applying stepwise, the proposed snow module and monthly parameterization during the validation period. Further testing and verification for model overfitting are also presented in this section. Finally, the calibrated monthly parameters are presented and discussed as well. The results of the stepwise improvements in model performance are summarized in Table 1.

### 4.1. Performance of the Original ZDWBM Across the Continental United States

The performance of the original ZDWBM varied greatly by region across the CONUS (Figure 4a). The cumulative distribution function (CDF) of ZDWBM's NSE values shows that the model performance is *good* for 38% of the 1,210 HCDN catchments (Figure 4b). As expected, the model confronts evident limitations in areas affected by snow, including high elevation catchments located in the Rocky Mountains area (HUC2 regions 13, 14, 15, 16, and 17) and catchments in the northern CONUS (HUC2 regions 1, 4, 7, and 9), likely due to its exclusion of a snow process representation (Figure 4c). The degradation of model performance with increasing snow-factor index confirms the absence of snow components in the model (Figure 4d). This result is consistent with a previous study that explored the monthly hydroclimatology of the CONUS with ZDWBM (Petersen et al., 2018). The median NSE value of the model across all the 1,210 catchments is estimated as  $\sim 0.5$ , while it is  $\sim 0.3$  in snow-affected regions ( $R > 0.4$ ).

### 4.2. Model Performance With the Implanted Snow Module

After implanting the proposed snow module in ZDWBM (ZDWBM-snow), the model shows a significant improvement in estimating monthly streamflow, especially for snow-affected regions (Figure 5a). The median NSE value of ZDWBM-snow for the CONUS shows a slight improvement ( $\sim 0.1$ ), whereas it improves considerably from  $\sim 0.3$  to  $\sim 0.5$  for snow-affected regions. It can be seen from Figures 5a and 5c that the model performance improves the most in the Northeastern region (HUC2 regions 1 and 2) and Rocky Mountains region (HUC2 regions 14, 16, and 17). Compared to the results from the original ZDWBM, the median values of NSE in those areas increase to 0.31 on average, and the variance reduces remarkably with ZDWBM-snow. Stations where ZDWBM-snow shows good performance accounted for 39% of the total (Figure 5b), as opposed to 33% of the total for the original ZDWBM. As presented in Figure 5d, the association between the NSE values and snow-runoff

**Table 1**  
Summary of the Incremental Improvements of the Model for All and Snow-Affected HCDN Catchments Across the CONUS

	Total HCDN catchments		
	Original ZDWBM	Model with snow module	Model with snow module and monthly parameters
Median NSE	0.51	0.61	0.67
Evaluation (%)			
Good	33	39	56
Satisfactory	19	28	26
Unsatisfactory	48	33	18
Overall Bias (%)	3	3	1
Seasonal Bias (%)			
Winter	−3	11	5
Spring	26	13	−5
Summer	−7	−10	5
Fall	−31	−29	4
	Snow-Affected HCDN Catchments ( $R > 0.4$ )		
	Original ZDWBM	Model with Snow Module	Model with Snow Module and Monthly Parameters
Median NSE	0.27	0.47	0.64
Evaluation (%)			
Good	3	15	48
Satisfactory	13	32	33
Unsatisfactory	84	53	19
Overall Bias (%)	5	5	2
Seasonal Bias (%)			
Winter	−33	20	13
Spring	37	14	−4
Summer	2	−6	2
Fall	−36	−29	8

Note. Positive bias indicates model is underestimating the flow, whereas negative bias indicates model is overestimating. See Section 4.2 for details.

ratio index  $R$  mostly diminishes after applying the snow module. Nevertheless, ZDWBM-snow still underperforms overall, showing NSE values  $\leq 0.5$  for 33% of the total catchments, especially in the northern part of the Midwest region (HUC2 regions 4 and 9), where the catchments are heavily influenced by snow. This indicates that the model is not yet adequately capturing the hydrological process, including the complicated melting mechanism, for some areas where snow is dominantly affecting the local water balance. There could be several aspects to consider in explaining these remaining errors. However, the most attributable factor is the single-value parameterization for describing the catchment's hydrological characteristics that can often vary from season to season.

Percent bias is one of the evaluation statistics that measure simulated flow's average tendency to be larger or smaller than their corresponding observed data (Gupta et al., 1999). Low magnitudes indicate accurate model estimation. Positive bias indicates that the model is underestimating the flow, whereas negative values indicate overestimation. The seasonal bias values of the ZDWBM-snow across all the 1,210 basins are 11%, 13%, −10%, and −29% for winter, spring, summer, and fall, respectively. The snow-affected regions show 20%, 14%, −6%, and −29% bias for each season from winter to fall, respectively (Figure 6).

Histograms of the relative errors between the observed and simulated flows exhibit right-skewed distributions every season for both groups, as is expected of data which is bounded on the left tail. The lower limit of relative error is mathematically −1, while the upper bound is unlimited. From these results, we argue that, on average, the ZDWBM-snow tends to underestimate the streamflow during winter and spring and overestimate during summer

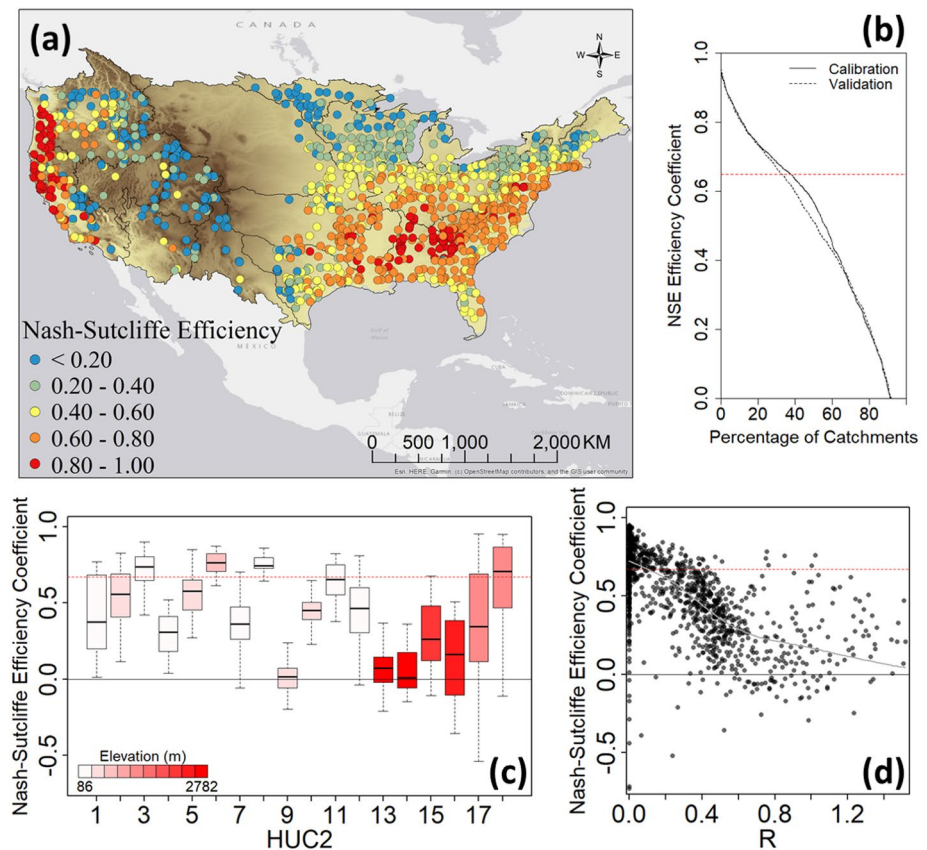


**Figure 4.** Performance of the original ZDWBM across the CONUS: (a) spatial distribution of NSE across the CONUS (b) cumulative distribution function of NSE (c) distribution of NSE for each HUC2 region (d) dependence between NSE and the snow-factor  $R$ . The red horizontal dashed line in each subfigure indicates the threshold for a good model ( $NSE > 0.65$ ).

and fall for the catchments across CONUS. For snow-affected regions, the model underestimates monthly streamflow during winter and spring and overestimates during fall. This seasonal bias is assumed as an error-offsetting result since the model's calibration process is designed to minimize the overall error with time-invariant parameters, expected to represent the catchment's hydrological characteristics.

In practice, for example, the melting efficiency ( $\beta$ ) of a watershed should be relatively low during snow accumulation seasons but high in snow melting seasons. However, during the calibration process, the model determines a single-valued optimal  $\beta$  to minimize the overall error between the simulated and observed flows. This "time-invariant calibration" causes  $\beta$  to be overestimated for snow accumulation seasons and underestimated for snow melting seasons. This type of seasonal bias can also occur due to the other model parameters ( $\alpha_1, \alpha_2, d, S_{max}$ ) as long as they are introduced as time-invariant values. Even if the true values of parameters are nearly constant, changing very little over time, streamflow can be highly sensitive to those small changes. Therefore, we reckon single-value parameters are insufficient to fully account for the temporal variability of the catchment's hydrological characteristics.

#### 4.3. Model Performance With the Implanted Snow Module and Monthly Parameterization

ZDWBM-snow is calibrated against observed streamflow data with five parameters ( $\alpha_{1n}, \alpha_{2n}, d_n, S_{maxn}$ , and  $\beta_n$ ) that vary over the 12 months ( $n = 1 : 12$ ). The model performance significantly improves when a combination of the snow module and monthly parameterization is applied. Except for a few, most catchments across the CONUS show a good agreement between the simulated flow and observed flow according to the computed NSE coefficients (Figure 7a). The median NSE values for CONUS and snow-affected regions are both  $\sim 0.65$ . The accuracy of the monthly calibrated ZDWBM-snow (ZDWBM-msnow) is evaluated to be *good* for 56% of the total HCDN

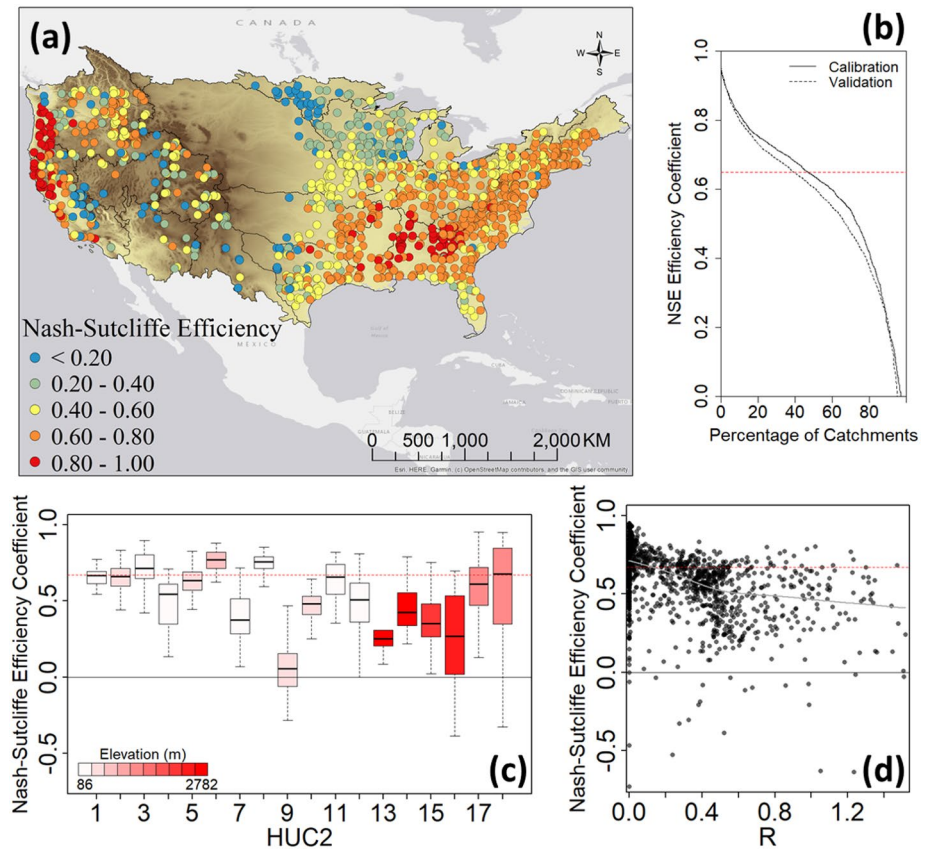


**Figure 5.** Performance of ZDWBM-snow across the CONUS: (a) spatial distribution of NSE across the CONUS (b) cumulative distribution function of NSE (c) distribution of NSE for each HUC2 region (d) dependence between NSE and the snow-factor index  $R$ . The red horizontal dashed line in each subfigure indicates the threshold for a good model ( $NSE > 0.65$ ).

catchments (Figure 7b). According to Figure 7c, catchments in HUC2 regions 9 and 15 tend to show relatively poor model performances than others. Both the elevation and snow-runoff ratio now show little effect on the model performance (Figures 7c and 7d).

Compared to the model without monthly parameterization, ZDWBM-msnow shows significantly lower bias for catchments across the CONUS, including the areas affected by snow, regardless of the season (Figure 8). Across the 1,210 catchments, the model bias is estimated as  $-5\%$ ,  $-5\%$ ,  $5\%$ , and  $4\%$  for each season, respectively, from winter to fall. Compared to the previous biases ( $11\%$ ,  $13\%$ ,  $-10\%$ , and  $-29\%$ ), both the magnitude and seasonal variance of the bias have decreased. The bias for snow-affected catchments also shows relatively small magnitudes than before through winter to fall, estimated as  $13\%$ ,  $-4\%$ ,  $2\%$ , and  $8\%$ , respectively. This is considered a promising improvement, given the previous biases for the corresponding catchments are  $20\%$ ,  $14\%$ ,  $-6\%$ , and  $-29\%$ , respectively.

#### 4.4. Assessment and Verification of the Model Improvements

The results clearly show that the model performs better after applying the proposed methods. The median NSE increases to  $\sim 0.7$  from  $\sim 0.5$  for all the catchments, and only 18% of them show  $NSE \leq 0.5$ . Catchments with the most significant improvements in model performance are hydrologically snow-dominated ( $R > 0.5$ ), while catchments moderately affected by snow ( $0.4 < R \leq 0.5$ ) show marginal improvements (Figure 9). The median NSE of the original model for snow-dominated catchments was  $\sim 0.3$ , and this dramatically increases to  $\sim 0.6$  with ZDWBM-msnow. Whereas the original model was evaluated as *unsatisfactory* ( $NSE \leq 0.5$ ) for 84% of these catchments, ZDWBM-msnow underperforms in only 19% of them. For most of the basins where snow is not considered an important local water source ( $R \leq 0.4$ ), the final model shows a slightly better, or at least

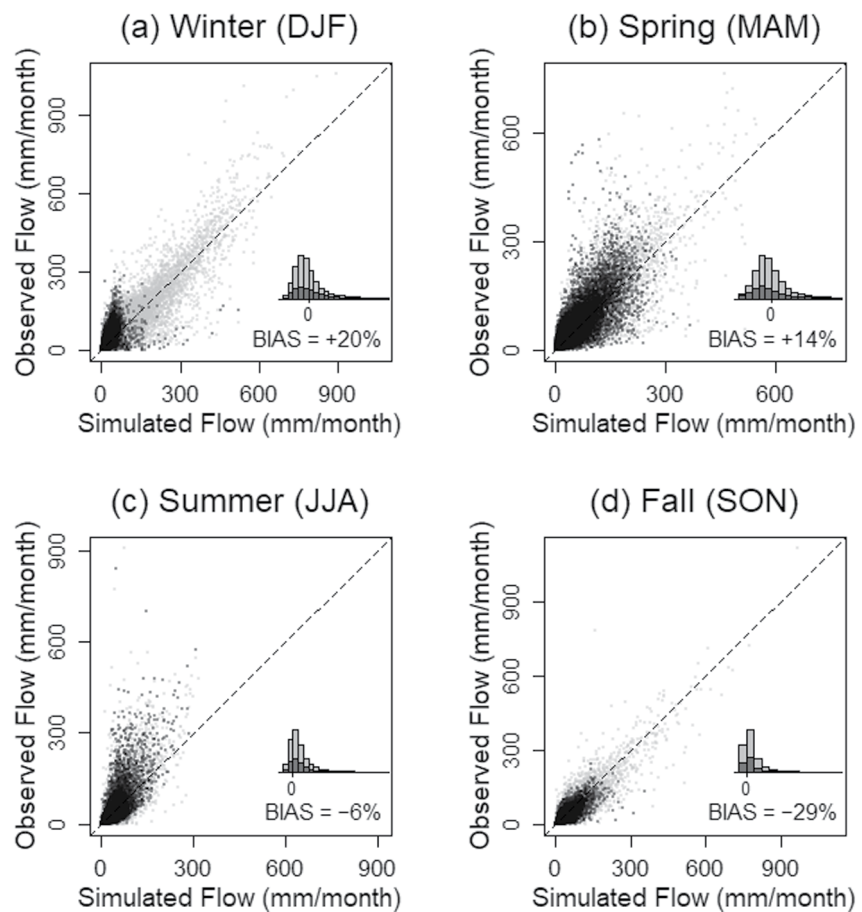


**Figure 6.** Bias of ZDWBM-snow for each season. The data points shown in gray indicate catchments that are less affected by snow ( $R \leq 0.4$ ), whereas the data points shown in black are snow-affected basins ( $R > 0.4$ ). The inset of each subfigure represents the histogram of relative errors between the observed and simulated for all catchments (gray) and snow-affected catchments (black).

similar, performance compared to the original model, with few exceptions. Most of these exceptions happen in catchments less affected ( $R \leq 0.4$ ) or dominated ( $R > 0.5$ ) by snow. The degradation of the model performance in these catchments could be due to the misallocation of available energy for melting.

As ZDWBM-msnow includes a snow module with an increased number of parameters due to the monthly parameterization, the model's complexity increases, and thus we cross-validate the model to test overfitting. Overfitting tends to occur when the model is unnecessarily complex, incorporating unnecessary processes (Vanlier et al., 2014), and when it contains an excessive number of parameters (Orth et al., 2015). The problem of overfitted models lies in the fact that they try to fit the random noise rather than only the signal. It typically shows a remarkable performance during the calibration stage and seems to capture the underlying hydrological process accurately, but it exhibits significant performance degradation during the validation period.

We only focus on 636 catchments for the cross-validation test, where 37 years of continuous observed streamflow data are provided. After calibrating the model against the first 19 years (~50% of 37 years) of data (training set), the model is validated with the later 18 years (testing set). When the intercept is set to zero, the overall  $R^2$  of the regression of calibrated NSE on simulated NSE is calculated as 0.87 (Figure A1a), indicating a good correspondence between calibrated NSE and simulated NSE. Besides, the slope of the fitted line is 1.040 with a 0.016 standard error. For a cross-validation test, it is ideal to have the points settled on the fitted line with a slope of 1 and an intercept of 0. Most of the tested results here are adjacent to the 1:1 line, except for a few cases. The percentage of catchments where the model showed a *good* performance was greater during the calibration period than the validation period, and the distributions of NSE values were slightly different from each other

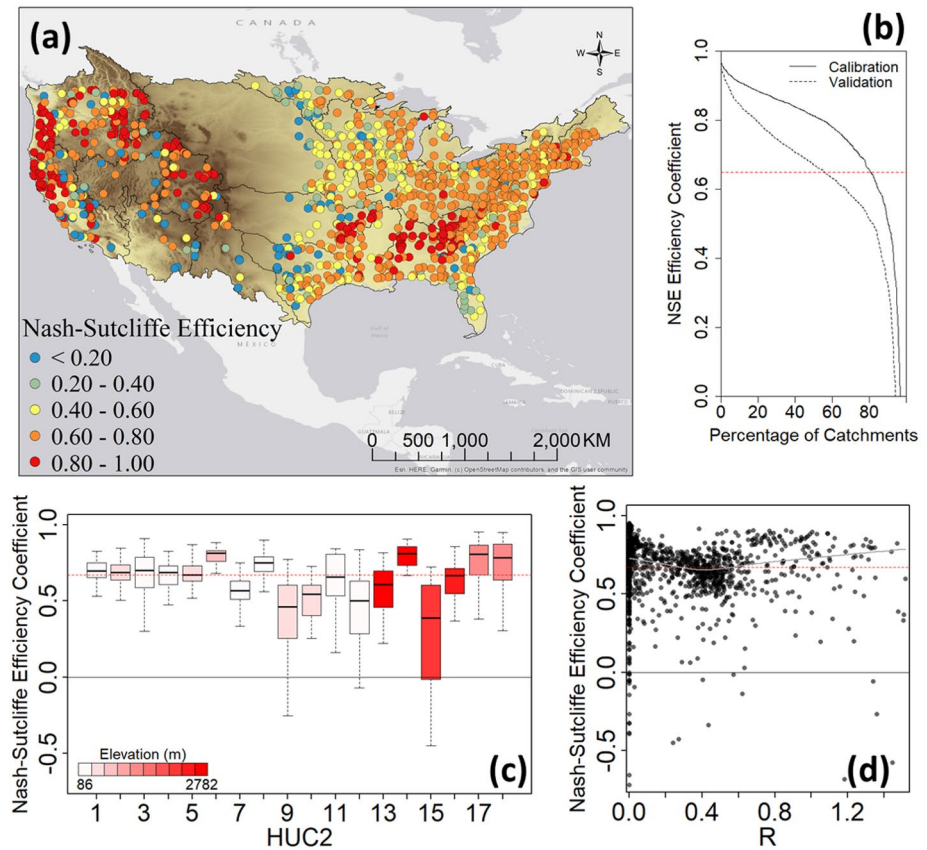


**Figure 7.** Performance of ZDWBM-msnow across the CONUS: (a) spatial distribution of NSE across the CONUS (b) cumulative distribution function of NSE (c) distribution of NSE for each HUC2 region (d) dependence between NSE and snow-factor index  $R$ . The red horizontal dashed line in each subfigure indicates the threshold for a good model ( $NSE > 0.65$ ).

(Figure A1b). This level of model deficiency during the testing period is expected as the model training involves observed streamflow while testing is blind to the observed. Overall, the differences between the calibration and validation results lie within the range that could be expected, and thus we conclude the proposed model does not show a concerning level of overfitting.

#### 4.5. Assessment of Model Parameters

Here we explore the spatial and seasonal variability of the parameters that are estimated by calibrating ZDWBM-msnow for the entire observed data (Figure 10). To ensure that the interpretations are reasonable, we only consider catchments where the model calibration is evaluated as *good*. This selection provided us 1,008 HCDN basins across CONUS for further investigation. Monthly parameters are explored based on the four seasons by averaging the monthly values corresponding to each season: winter (December–February), spring (March–May), summer (June–August), and fall (September–November).

The melting efficiency ( $\beta_n$ ) displays a significant seasonality for most of the catchments, as anticipated. During the winter season, groups of catchments with the highest values of  $\beta_n$  are located in the Pacific Coast and southern part of the CONUS. As spring comes,  $\beta_n$  starts to increase in catchments located northbound of the South and Southeast region, and this increase of  $\beta_n$  continues northward as summer approaches. When summer arrives, most of the catchments in the CONUS have high melting efficiency ( $0.8 < \beta_n$ ), and this state is maintained until fall.

The catchment retention efficiency ( $\alpha_{1n}$ ) shows a seasonal variability for some catchments across the CONUS. During winter and spring, the eastern CONUS generally shows lower  $\alpha_{1n}$  values than the western CONUS, but this relation overturns in summer and fall. Especially during the spring season, the Northeast and Ohio Valley (HUC2 region 5) regions display particularly low  $\alpha_{1n}$  values. Since  $\alpha_{1n}$  describes catchment retention, this cluster

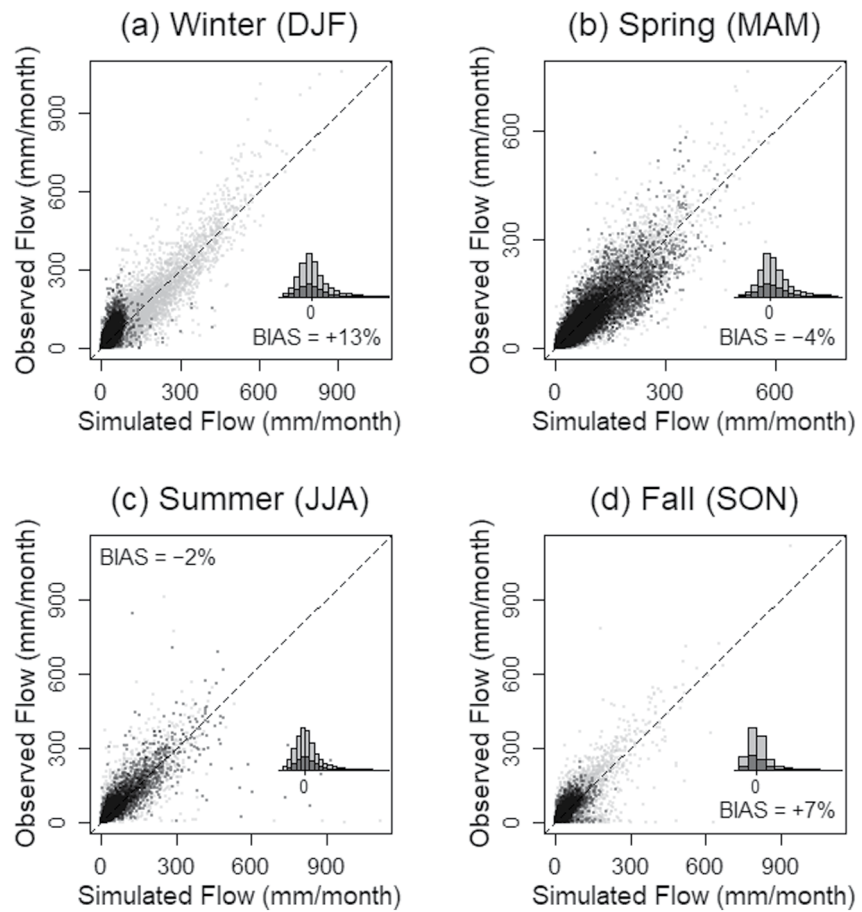


**Figure 8.** Bias of ZDWBM-msnow for each season. The data points shown in gray indicate catchments that are less affected by snow ( $R \leq 0.4$ ), whereas the data points shown in black are snow-affected basins ( $R > 0.4$ ). The inset of each subfigure represents the histogram of relative errors between the observed and simulated for all catchments (gray) and snow-affected catchments (black).

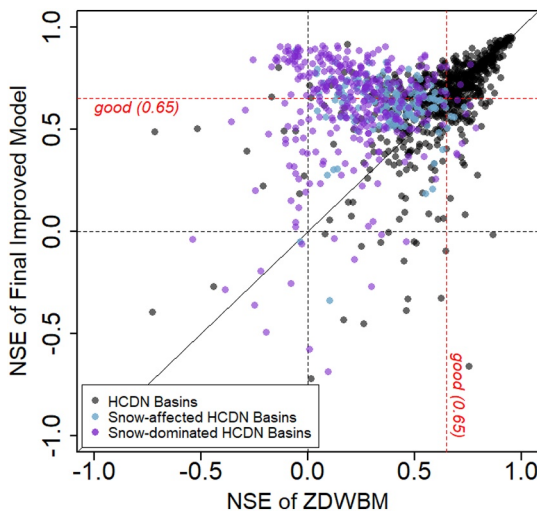


**Figure 9.** Comparison of NSE for ZDWBM-msnow and original ZDWBM. For clarity, NSE values less than  $-0.75$  are chosen as lower outliers and omitted from the figure. These are  $\sim 3\%$  of all the 1,210 stations.

of low  $\alpha_1$  in spring may imply a low infiltration rate and intense water supply, indicating more direct runoff in the area. We assume this is strongly related to snowmelt in spring. The evapotranspiration efficiency ( $\alpha_{2n}$ ) shows varying peak timings for different regions across the CONUS. The South and Ohio Valley regions show quasi-constant  $\alpha_{2n}$  values  $\sim 0.6$ – $0.8$  regardless of the seasons. Meanwhile, the Pacific Coast near California shows highest  $\alpha_{2n}$  during the spring season and lowest during summer and fall. The rest of the catchments mostly show highest  $\alpha_{2n}$  during the summer season, especially those located in the Northeast, Pacific Northwest, and Upper Midwest regions. A previous study argues that  $\alpha_{2n}$  is heavily related to various climate factors, such as precipitation, aridity index, peak-lags between precipitation and evapotranspiration, and coefficient of variation of precipitation (Hamel et al., 2017). In fact, the spatial distribution of  $\alpha_{2n}$  displays a similar pattern to the aridity index gradient of the CONUS (Petersen et al., 2012).

The groundwater transition rate ( $d_n$ ) displays a strong spatial and seasonal variability for the catchments across the CONUS. Most of the catchments have a low to moderate value of  $d_n$  during winter. The  $d_n$  values generally increase as spring arrives and reaches the peak for most catchments, except for those located in the Upper Midwest region. During the summer season,  $d_n$

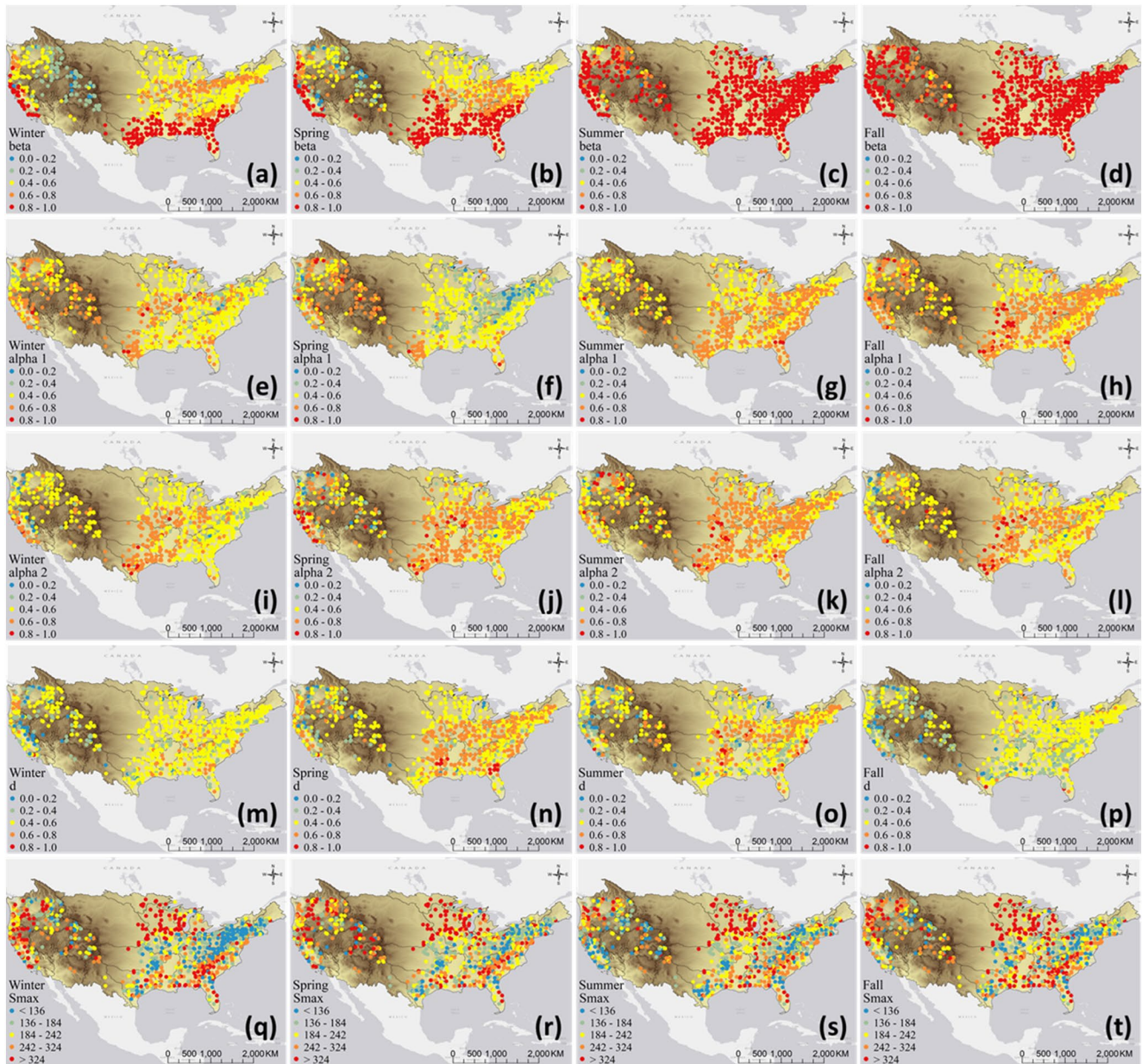


**Figure 10.** Seasonal spatial distribution of average melting efficiency (a–d), catchment retention efficiency (e–h), evapotranspiration efficiency (i–l), groundwater transition rate (m–p), and maximum soil-moisture capacity (q–t) for the HCDN catchments where ZDWBM-msnow performance was classified as *good* during the calibration.

decreases at some catchments, including the Tennessee Valley (HUC2 region 6) and Pacific Coast, but remains at a similar level from spring for most catchments. Then the majority of the catchments show a decrease in  $d_n$ , having their lowest  $d_n$  values in fall.

The maximum soil-moisture storage capacity ( $S_{max}$ ) is consistently high in the Midwest region and northbound of the Southeast region, while being relatively low in the Ohio Valley and Northeast regions throughout the four seasons. Catchments in close proximity to the Rocky Mountains Range, including those in California, have lowest  $S_{max}$  in summer.

## 5. Discussion

### 5.1. Comparison With Previous Studies

The combined results from Figure 4 indicate that the original ZDWBM is noticeably inadequate for the CONUS. A previous study has demonstrated that the model was well validated when tested for catchment in Australia, with NSE values ranging from 0.6 to 0.9 for the majority (L. Zhang et al., 2008). The study used unimpaired streamflow data that was modeled without considering snowmelt water (Peel et al., 2000), which is reasonable since snow does not play a significant role in the hydrology of those tested catchments, except for a few high elevation areas in the southeast Australia and Tasmania region (Q. J. Wang et al., 2011). However, the hydrology of a large area in the CONUS is under the influence of snowmelt water to such an extent that more than 40% of the total HCDN catchments are snow-affected ( $R > 0.4$ ). Evidently, the lack of snow process representation leads to the underperformance of the model for the CONUS.

ZDWBM-msnow shows an excellent performance in simulating runoff at snow affected areas compared to the original ZDWBM and other monthly water balance models with snow module. Martinez and Gupta (2010) tested the augmented *abcd*-snow model on 764 HCDN catchments across the CONUS. The model includes a simple temperature-based snow component and requires a preprocessing classification of catchments into “snow” or “no snow” based on whether snow accumulation/melt dynamics play an important role. The model performed well during the calibration process but only ~31% of the total tested catchments showed  $NSE > 0.67$  during validation. Particularly, only ~18% of the “snow” catchments showed  $NSE > 0.67$ . It is difficult to make a direct comparison since the settings are different, but ZDWBM-msnow shows  $NSE > 0.67$  for ~50% of the tested catchments and ~43% of snow-affected catchments. Bock et al. (2016) also applied a monthly water balance model (MWB) that is based on a simple concept of water supply and demand (McCabe & Markstrom, 2007) to the CONUS. This model also contains a snow module that involves a partitioning process of precipitation into rainfall and snowfall based on temperature thresholds. In MWB, snow is accumulated in a snowpack, and the amount of snowmelt is controlled by a model parameter that determines the proportion of snowpack that melts. The MWB showed a median NSE of 0.76 across the CONUS, but the model performance in high latitudes, high plains, and desert southwest was less promising. These areas are coherent with those where the original ZDWBM and ZDWBM-snow show poor performance. However, the estimations of runoff in those areas are significantly improved by ZDWBM-msnow.

Various approaches have been established to better represent the snow dynamics considering its significant impact on hydrology. These approaches have been mostly based on either energy balance models or temperature-index models. Physics-based energy balance snow models, such as ISNOBAL (Marks et al., 1999), SNOWPACK (Lehning et al., 2002), SnowModel (Liston & Elder, 2006), and VIC (Andreaskis & Lettenmaier, 2006), have been widely used in the hydrology field as they allow full control over the detailed components of snow processes at the basin or grid scale. This type of modeling, however, requires a considerable amount of investment in data preparation and computation. Moreover, it is difficult to identify the source of errors when the model is too complicated. Temperature-index approaches are also popular for snow modeling because of their simplicity, especially when information other than temperature is lacking. However, classical temperature-index models sometimes fail to capture the underlying physics of the hydrological process because of its simplicity and its catchment scale and longer time scale assumptions (Lang & Braun, 1990). To the best of our knowledge, the snow module developed in this study is the first Budyko-type snow representation that incorporates surface energy balance. The snow module achieves parameter parsimony as it follows the supply-demand limit concept of Budyko's framework while being physically meaningful at the same time as it is based on the surface energy balance.

### 5.2. Limitations and Uncertainties

Overall, ZDWBM-msnow displays a superior performance compared to the original model in simulating monthly streamflow for 70% of the tested catchments across the CONUS. Monthly hydrographs for three randomly selected stations, each representing different snow conditions, demonstrate how ZDWBM-msnow better predicts the streamflow dynamics than the original ZDWBM and ZDWBM-snow (Figure A2). ZDWBM-msnow show little if any improvements in regions not affected by snow ( $R \leq 0.4$ ) but show a remarkable capability of capturing monthly high flow events compared to the original ZDWBM and ZDWBM-snow in snow regions ( $R > 0.4$ ). Only 18% of the total tested catchments show poor estimates ( $NSE < 0.5$ ) with ZDWBM-msnow.

These catchments tend to have shorter records of observation comparing to those where  $NSE \geq 0.5$  (Figure A3), which is reasonable since the length of observation influences the calibration efficiency of the model—that is, parameters calibrated based on more observational data better characterize basin properties. Moreover, these catchments with  $NSE < 0.5$  have drier conditions, lower values of snow-factor index  $R$ , and higher long-term mean temperatures than catchments with  $NSE \geq 0.5$  (Figure A4). All of these aspects are more likely to appear in arid regions than in humid areas. This finding is consistent with previous literature that argued parameter parsimonious monthly water balance models are capable to accurately simulate streamflow in humid regions (Guo et al., 2002; Vandewiele & Ni-Lar-Win., 1998; Xu & Singh, 1998), but less promising in arid regions (Atkinson et al., 2002; Hu et al., 2005; Xu & Singh, 1998). The additional layer of water storage (i.e., snowpack) provided by the snow module could be one of the chief factors degrading the model performance in arid regions. The snow module is based on several assumptions that may bring small perturbations into the estimated snowpack, and dry catchments usually show high sensitivity to the storage components, producing runoff predictions with little confidence (Atkinson et al., 2002; C. Wu et al., 2018).

Despite the significant improvements that were shown in this study, ZDWBM-msnow may still have some limitations due to some of its assumptions. The snow mass balance in this study neglects snow sublimation during both the snow accumulation and melting periods. However, sublimation of snow and ice sometimes can be a significant component for the snow mass balance (MacDonald et al., 2010; Reba et al., 2012; Strasser et al., 2008). Since snowmelt is an extremely important source of water (Barnett et al., 2005; Pierson et al., 2013; Viviroli et al., 2011), these snow sublimation losses can significantly affect the water balance, especially in the snow affected regions. The neglected snow sublimation losses could possibly be interpreted as errors in the other water balance components of ZDWBM-msnow during snow accumulation and melting periods. Correspondingly, low NSE values of ZDWBM-msnow are observed at some of the mountainous and northern end regions of the CONUS (Figure 7a), which are particularly cold in winter, likely due to the lack of snow sublimation accounting.

In reality, negative radiation balance can be observed during snow accumulating seasons or in regions of permanent snow and ice cover. However, our estimated net radiation heat flux is assumed to be always positive since the calculations are based on a dataset of positive-only potential evapotranspiration estimates from the Hargreaves method. This leaves latent heat from condensation and freezing neglected, inducing the model to have potential errors for certain catchments under the influence of snow. Additionally, the rough estimate of total energy available for potential evapotranspiration and potential melting is expected to affect the model accuracy.

### 5.3. Effect of the Snow Module on ET Estimation

One of the main features of the snow module developed in this study is the newly computed  $PET$  and potential melting,  $PM$ , based on surface energy balance and Budyko's framework. As Budyko-based estimates of  $ET$  are controlled by  $P$  and  $PET$ , the newly computed  $PET$  is expected to have direct effects on  $ET$  estimates. A comparison of  $ET$  estimates between ZDWBM and ZDWBM-msnow for snow-affected regions ( $R > 0.4$ ) indicates that the inclusion of snow module and monthly parameterization results in lower  $ET$  estimations in winter and higher  $ET$  estimates in summer (Figure A4). ZDWBM-msnow shows lower winter  $ET$  values than ZDWBM because ZDWBM-msnow separates precipitation into rainfall and snowfall during the snow accumulating and melting phases, and thus the amount of water contents available for  $ET$  decreases. The total energy flux available for phase changes are also partially allocated to  $PM$  in ZDWBM-msnow, resulting in less energy available for  $PET$ . Moreover, the amount of water leaving the system as  $ET$  in ZDWBM could be partially stored in the form of snowpacks during the winter season in ZDWBM-msnow. In summer, ZDWBM-msnow yields higher  $ET$  values than ZDWBM because snowpacks from the antecedent seasons (winter and spring) provide water inputs to the catchment, enabling more  $ET$  to occur. In addition, ZDWBM tends to preserve more water in summer by yielding small  $ET$  estimates in order to recover the water loss due to  $ET$  overestimation that occurred in the previous winter.

The choice of  $PET$  method could be one of the key factors that determine the performance of ZDWBM-msnow since the snow module is based on the estimated  $PET$  values. The performance of  $PET$  methods may differ by region and catchment condition as they are developed with different approaches (Federer et al., 1996; Lu et al., 2005). Several past studies tested the impact of different  $PET$  methods on the performance of water balance models, and it was revealed that the choice of  $PET$  method has a low influence on runoff estimations (Aouissi et al., 2016; P. Bai et al., 2016). Simple potential evapotranspiration methods that are based on extraterrestrial ra-

diation and air temperature, such as the Hargreaves method, are shown to be as efficient as more complex models for catchment scale water balance models (Oudin et al., 2005). However, it was also shown that different potential evapotranspiration methods might affect the parameter calibration of hydrological models (P. Bai et al., 2016). By determining the most effective *PET* method for each target region, therefore, the accuracy of model parameters estimation may be enhanced.

## 6. Summary and Conclusion

This study explores the limitations of an existing dynamic water balance model (ZDWBM) proposed by L. Zhang et al. (2008). It provides measures to overcome those limits based on more than 1,200 unmodified basins across the CONUS with observation data of 31 years on average. Zhang's dynamic water balance model (ZDWBM) describes the monthly water balance of a catchment by partitioning the hydrological process based on Budyko's framework. While this model showed a quality performance for catchments in Australia (L. Zhang et al., 2008), it fails to perform well for the catchments in the CONUS. The model mainly shows lower performance in snow-affected basins as it does not contain snow components. This limitation of the model is critical when applied to the CONUS since a significant portion of its catchments is affected by snow. The model suits only 57% of the given catchments and 18% of the snow-affected regions.

A snow module is developed in this study to improve the model applicability to the CONUS. The snow module is designed based on the concept of Budyko's framework to preserve the spirit and parameter parsimony that ZDWBM has achieved. The augmented model with snow module shows a significant improvement in simulating monthly streamflow, especially for snow-affected regions. However, we find the augmented model produces a seasonal bias in the simulated streamflow, requiring an additional improvement strategy. We assume the model's seasonal bias is attributable to the time-invariant model parameters inaccurately representing the time-varying catchment characteristics. In order to minimize the seasonal bias, the snow augmented model is calibrated with monthly parameters (ZDWBM-msnow). After applying monthly parameterization to the snow augmented model, it becomes suitable for more than 90% of the total catchments, and the seasonal bias diminishes.

Based on the ZDWBM-msnow, we also discussed the catchment's hydrological characteristics across the CONUS by assessing the spatial variability of the model parameters for each season. For each model parameter, catchments with similar values are regionally grouped as various clusters in general. While catchment melting efficiency ( $\beta_n$ ), retention efficiency ( $\alpha_{1,n}$ ), evapotranspiration efficiency ( $\alpha_{2,n}$ ), and groundwater transition rate ( $d_n$ ) display seasonal variations in most catchments, the maximum soil-moisture storage capacity ( $S_{max,n}$ ) shows only small changes over the four seasons. Further investigations could be conducted to better understand the factors that control the spatiotemporal variability of the parameters.

Since the model parameters are related to the hydrological characteristics of a catchment, a further investigation on the model parameters and catchment characteristics could be conducted to predict the streamflow response to changes in land-use/land cover for catchments, including those ungauged. A successful analysis of the relationship between catchment characteristics and the model parameters will provide further physical interpretation and allow easy applicability for decision-making for various purposes, such as water resources management, restoration of ecological flow, and water-relevant policymaking.

Our analyses suggest that ZDWBM-msnow could be used to estimate monthly runoff for ungauged basins across the continental United States. Regionalization of model parameters will be a prerequisite for this usage, and thus one may consider modeling the parameters of ungauged basins based on their regional climate and catchment characteristics. Hamel et al. (2017) model the parameters of the original ZDWBM based on a set of climate and catchment characteristics for Australian basins, and the modeled parameters show a good performance predicting dry-season flow. This could be analogously applied to the US basins in future studies by using ZDWBM-msnow. For this purpose, one may also consider redesigning ZDWBM-msnow using a Bayesian hierarchical structure to enhance the parameter estimation procedure and better represent their uncertainties. By pooling the parameters over similar geospatial catchments, a Bayesian hierarchical approach can provide improved model parameter estimations with reduced uncertainty. Moreover, it will also provide information of the uncertainty level of the simulated streamflow which could be used in water systems' decision analyses.

Appendix A

Figures A1–A4

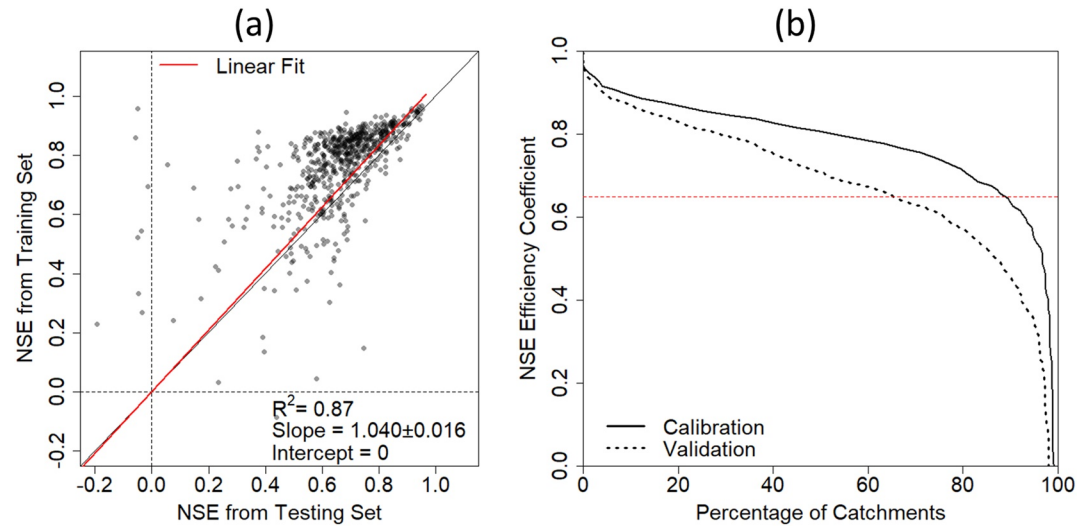


**Figure A1.** Cross-validation results verifying for overfitting. (a) Comparison between NSE from calibration and validation periods. (b) Comparison between the cumulative distribution function of NSE from calibration (solid) and validation periods (dotted).

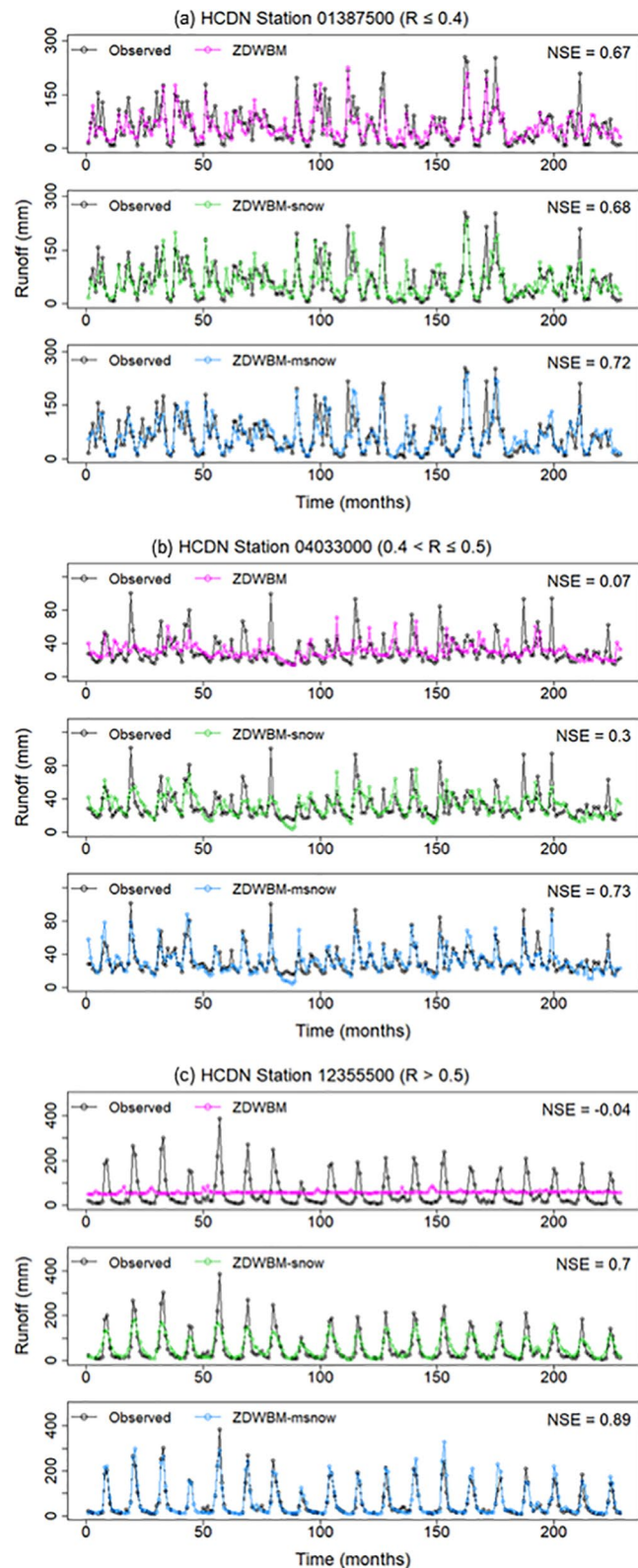


**Figure A2.** (a) Monthly hydrographs estimated with ZDWBm (top), ZDWBm-msnow (middle), and ZDWBm-msnow (bottom) for a randomly selected HCDN basin less affected by snow ( $R \leq 0.4$ ). (b) Monthly hydrographs estimated with ZDWBm (top), ZDWBm-msnow (middle), and ZDWBm-msnow (bottom) for a randomly selected HCDN basin moderately affected by snow ( $0.4 < R \leq 0.5$ ). (c) Monthly hydrographs estimated with ZDWBm (top), ZDWBm-msnow (middle), and ZDWBm-msnow (bottom) for a randomly selected HCDN basin dominated by snow ( $R > 0.5$ ).

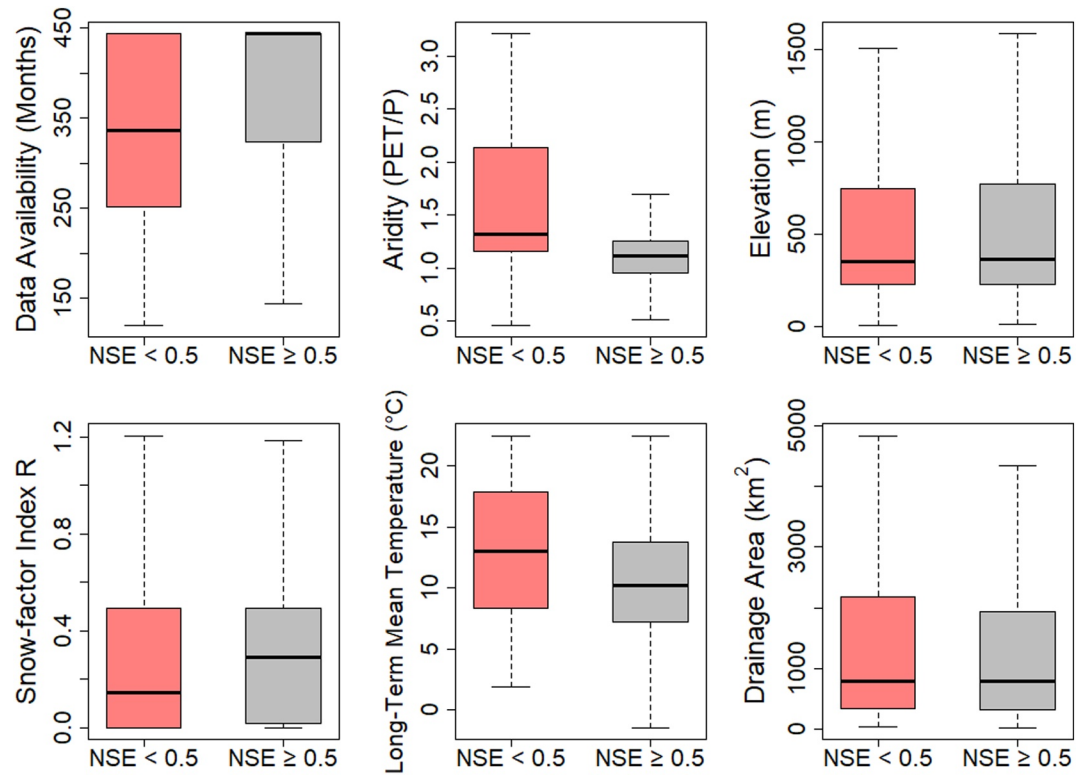


**Figure A3.** Characteristics comparison between catchments with  $NSE < 0.5$  and  $NSE \geq 0.5$ .

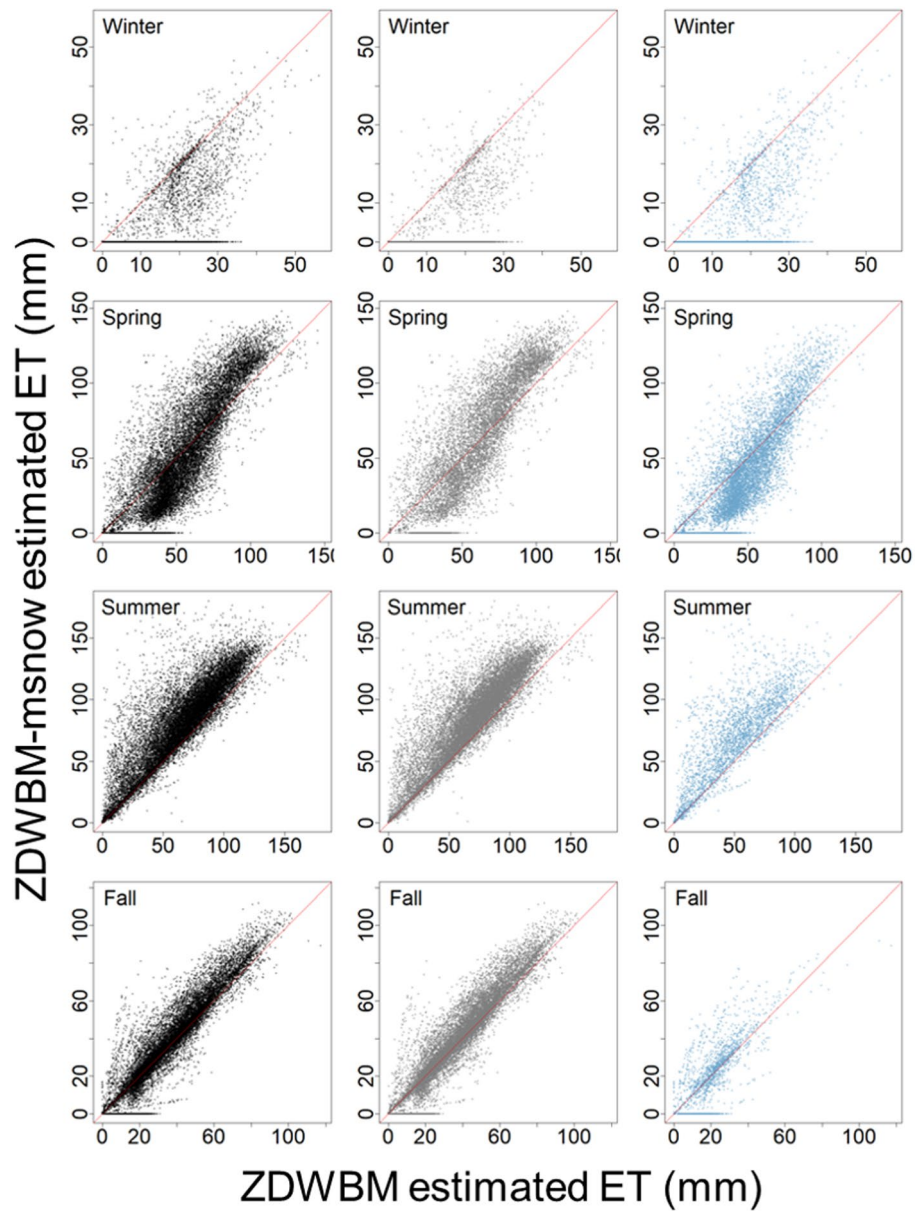


**Figure A4.** Comparison of estimated ET between ZDWBm-*msnow* and ZDWBm for each season in snow-affected regions. The subplots in the first column show the full set of estimated monthly ET (black dots). The subplots in the second column show the estimated monthly ET for months snowpack is not presented (gray dots). The subplots in the third columns show the estimated monthly ET for months snowpack is presented (blue dots).

### Data Availability Statement

The monthly climate data for HCDN sites may be obtained from *Oak Ridge National Laboratory* (2015): Available at: [https://daac.ornl.gov/HYDROCLIMATOLOGY/guides/hcdn\\_monthly\\_hydroclim.html](https://daac.ornl.gov/HYDROCLIMATOLOGY/guides/hcdn_monthly_hydroclim.html). The monthly streamflow data for HCDN sites may be obtained from *U.S. Geological Survey* (1994): Available at: <https://water.usgs.gov/GIS/metadata/usgswrd/XML/hcdn.xml>. The estimated parameters from all three model types can be obtained from Dataverse: Available at: <https://doi.org/10.7910/DVN/BEZ8VR>.

## Acknowledgments

This work is supported by the U.S. Department of Energy Early CAREER Award No. DE-SC0018124 (PI. Naresh Devineni).

## References

- Anderson, M. G., & Burt, T. P. (1985). *Modelling strategies. Hydrological forecasting* (pp. 1–13). John Wiley and Sons.
- Andreadis, K. M., & Lettenmaier, D. P. (2006). Assimilating remotely sensed snow observations into a macroscale hydrology model. *Advances in Water Resources*, 29(6), 872–886.
- Andreadis, K. M., Storck, P., & Lettenmaier, D. P. (2009). Modeling snow accumulation and ablation processes in forested environments. *Water Resources Research*, 45(5). <https://doi.org/10.1029/2008wr007042>
- Aouissi, J., Benabdallah, S., Chabaane, Z. L., & Cudenneq, C. (2016). Evaluation of potential evapotranspiration assessment methods for hydrological modelling with SWAT—Application in data-scarce rural Tunisia. *Agricultural Water Management*, 174, 39–51. <https://doi.org/10.1016/j.agwat.2016.03.004>
- Atkinson, S. E., Woods, R. A., & Sivapalan, M. (2002). Climate and landscape controls on water balance model complexity over changing time-scales. *Water Resources Research*, 38(12), 50–51. <https://doi.org/10.1029/2002wr001487>
- Bai, J., Li, J., Shi, H., Liu, T., & Zhong, R. (2018). Snowmelt water alters the regime of runoff in the arid region of northwest China. *Water*, 10(7), 902. <https://doi.org/10.3390/w10070902>
- Bai, P., Liu, X., Liang, K., & Liu, C. (2015). Comparison of performance of twelve monthly water balance models in different climatic catchments of China. *Journal of Hydrology*, 529, 1030–1040. <https://doi.org/10.1016/j.jhydrol.2015.09.015>
- Bai, P., Liu, X., Yang, T., Li, F., Liang, K., Hu, S., & Liu, C. (2016). Assessment of the influences of different potential evapotranspiration inputs on the performance of monthly hydrological models under different climatic conditions. *Journal of Hydrometeorology*, 17(8), 2259–2274. <https://doi.org/10.1175/jhm-d-15-0202.1>
- Barnett, T. P., Adam, J. C., & Lettenmaier, D. P. (2005). Potential impacts of a warming climate on water availability in snow-dominated regions. *Nature*, 438(7066), 303–309. <https://doi.org/10.1038/nature04141>
- Beven, K., Lamb, R., Quinn, P., Romanowicz, R., & Freer, J. (1995). *Topmodel. Computer models of watershed hydrology* (pp. 627–668).
- Bock, A. R., Hay, L. E., McCabe, G. J., Markstrom, S. L., & Atkinson, R. D. (2016). Parameter regionalization of a monthly water balance model for the conterminous United States. *Hydrology and Earth System Sciences*, 20(7), 2861–2876. <https://doi.org/10.5194/hess-20-2861-2016>
- Boudhar, A., Boulet, G., Hanich, L., Sicart, J. E., & Chehbouni, A. (2016). Energy fluxes and melt rate of a seasonal snow cover in the Moroccan High Atlas. *Hydrological Sciences Journal*, 61(5), 931–943.
- Budyko, M. I. (1961). The heat balance of the earth's surface. *Soviet Geography*, 2(4), 3–13. <https://doi.org/10.1080/00385417.1961.10770761>
- Budyko, M. I., Miller, D. H., & Miller, D. H. (1974). *Climate and Life* (Vol. 508). Academic press.
- Chen, X., Alimohammadi, N., & Wang, D. (2013). Modeling interannual variability of seasonal evaporation and storage change based on the extended Budyko framework. *Water Resources Research*, 49(9), 6067–6078. <https://doi.org/10.1002/wrcr.20493>
- Daly, C., Neilson, R. P., & Phillips, D. L. (1994). A statistical-topographic model for mapping climatological precipitation over mountainous terrain. *Journal of Applied Meteorology and Climatology*, 33(2), 140–158. [https://doi.org/10.1175/1520-0450\(1994\)033<0140:astmfm>2.0.co;2](https://doi.org/10.1175/1520-0450(1994)033<0140:astmfm>2.0.co;2)
- Deng, C., Liu, P., Wang, D., & Wang, W. (2018). Temporal variation and scaling of parameters for a monthly hydrologic model. *Journal of Hydrology*, 558, 290–300. <https://doi.org/10.1016/j.jhydrol.2018.01.049>
- Duffie, J. A., & Beckman, W. A. (1980). *Solar engineering of thermal processes* (p. 16591). Wiley.
- Eagleson, P. S. (1978). Climate, soil, and vegetation: 1. Introduction to water balance dynamics. *Water Resources Research*, 14(5), 705–712. <https://doi.org/10.1029/wr014i005p00705>
- Ehret, U., & Zehe, E. (2011). Series distance—an intuitive metric to quantify hydrograph similarity in terms of occurrence, amplitude and timing of hydrological events. *Hydrology and Earth System Sciences*, 15(3), 877–896. <https://doi.org/10.5194/hess-15-877-2011>
- Farmer, D., Sivapalan, M., & Jothityangkoon, C. (2003). Climate, soil, and vegetation controls upon the variability of water balance in temperate and semi-arid landscapes: Downward approach to water balance analysis. *Water Resources Research*, 39(2). <https://doi.org/10.1029/2001wr000328>
- Fayad, A., Gascoïn, S., Faour, G., López-Moreno, J. I., Drapeau, L., Le Page, M., & Escadafal, R. (2017). Snow hydrology in Mediterranean mountain regions: A review. *Journal of Hydrology*, 551, 374–396. <https://doi.org/10.1016/j.jhydrol.2017.05.063>
- Federer, C. A., Vörösmarty, C., & Fekete, B. (1996). Intercomparison of methods for calculating potential evaporation in regional and global water balance models. *Water Resources Research*, 32(7), 2315–2321. <https://doi.org/10.1029/96wr00801>
- Fekete, B. M., Wisser, D., Kroeze, C., Mayorga, E., Bouwman, L., Wollheim, W. M., & Vörösmarty, C. (2010). Millennium ecosystem assessment scenario drivers (1970–2050): Climate and hydrological alterations. *Global Biogeochemical Cycles*, 24(4). <https://doi.org/10.1029/2009gb003593>
- Franks, S. W., Sivapalan, M., Takeuchi, K., & Tachikawa, Y. (2005). *Predictions in ungauged basins: International perspectives on the state of the art and pathways forward*. Food and Agriculture Organization of the United Nations (FAO).
- Fu, B. P. (1981). On the calculation of the evaporation from land surface. *Scientia Atmospherica Sinica*, 5(1), 23–31.
- Greve, P., Gudmundsson, L., Orlovsky, B., & Seneviratne, S. I. (2015). Introducing a probabilistic Budyko framework. *Geophysical Research Letters*, 42(7), 2261–2269. <https://doi.org/10.1002/2015gl063449>
- Guo, S., Wang, J., Xiong, L., Ying, A., & Li, D. (2002). A macro-scale and semi-distributed monthly water balance model to predict climate change impacts in China. *Journal of Hydrology*, 268(1–4), 1–15. [https://doi.org/10.1016/s0022-1694\(02\)00075-6](https://doi.org/10.1016/s0022-1694(02)00075-6)
- Gupta, H. V., & Kling, H. (2011). On typical range, sensitivity, and normalization of Mean Squared Error and Nash-Sutcliffe Efficiency type metrics. *Water Resources Research*, 47(10). <https://doi.org/10.1029/2011wr010962>
- Gupta, H. V., Sorooshian, S., & Yapo, P. O. (1999). Status of automatic calibration for hydrologic models: Comparison with multilevel expert calibration. *Journal of Hydrologic Engineering*, 4(2), 135–143. [https://doi.org/10.1061/\(asce\)1084-0699\(1999\)4:2\(135\)](https://doi.org/10.1061/(asce)1084-0699(1999)4:2(135))
- Hamel, P., Guswa, A. J., Sahl, J., & Zhang, L. (2017). Predicting dry-season flows with a monthly rainfall–runoff model: Performance for gauged and ungauged catchments. *Hydrological Processes*, 31(22), 3844–3858. <https://doi.org/10.1002/hyp.11298>
- Hamlet, A. F., Mote, P. W., Clark, M. P., & Lettenmaier, D. P. (2005). Effects of temperature and precipitation variability on snowpack trends in the western United States. *Journal of Climate*, 18(21), 4545–4561. <https://doi.org/10.1175/jcli3538.1>
- Hargreaves, G. H., & Samani, Z. A. (1982). Estimating potential evapotranspiration. *Journal of the Irrigation and Drainage Division*, 108(3), 225–230. <https://doi.org/10.1061/jrcea4.0001390>
- Harman, C., & Troch, P. A. (2014). What makes Darwinian hydrology "Darwinian"? Asking a different kind of question about landscapes. *Hydrology and Earth System Sciences*, 18(2), 417–433. <https://doi.org/10.5194/hess-18-417-2014>
- Hu, C., Guo, S., Xiong, L., & Peng, D. (2005). A modified Xinanjiang model and its application in northern China. *Hydrology Research*, 36(2), 175–192. <https://doi.org/10.2166/nh.2005.0013>
- Jensen, M. E., Burman, R. D., & Allen, R. G. (1990). *Evapotranspiration and irrigation water requirements*. ASCE.
- Koster, R. D., & Suarez, M. J. (1999). A simple framework for examining the interannual variability of land surface moisture fluxes. *Journal of Climate*, 12(7), 1911–1917. [https://doi.org/10.1175/1520-0442\(1999\)012<1911:asffet>2.0.co;2](https://doi.org/10.1175/1520-0442(1999)012<1911:asffet>2.0.co;2)

- Lang, H., & Braun, L. (1990). On the information content of air temperature in the context of snow melt estimation. *IAHS Publication*, 190, 347–354.
- Lehning, M., Bartelt, P., Brown, B., & Fierz, C. (2002). A physical SNOWPACK model for the Swiss avalanche warning: Part III: Meteorological forcing, thin layer formation and evaluation. *Cold Regions Science and Technology*, 35(3), 169–184. [https://doi.org/10.1016/S0165-232X\(02\)00072-1](https://doi.org/10.1016/S0165-232X(02)00072-1)
- Li, D., Pan, M., Cong, Z., Zhang, L., & Wood, E. (2013). Vegetation control on water and energy balance within the Budyko framework. *Water Resources Research*, 49(2), 969–976. <https://doi.org/10.1002/wrcr.20107>
- Liang, X., Lettenmaier, D. P., Wood, E. F., & Burges, S. J. (1994). A simple hydrologically based model of land surface water and energy fluxes for general circulation models. *Journal of Geophysical Research*, 99(D7), 14415–14428. <https://doi.org/10.1029/94jd00483>
- Liston, G. E., & Elder, K. (2006). A distributed snow-evolution modeling system (SnowModel). *Journal of Hydrometeorology*, 7(6), 1259–1276. <https://doi.org/10.1175/jhm548.1>
- Lu, J., Sun, G., McNulty, S. G., & Amatya, D. M. (2005). A comparison of six potential evapotranspiration methods for regional use in the south-eastern United States 1. *Journal of the American Water Resources Association*, 41(3), 621–633. <https://doi.org/10.1111/j.1752-1688.2005.tb03759.x>
- MacDonald, M. K., Pomeroy, J. W., & Pietroniro, A. (2010). On the importance of sublimation to an alpine snow mass balance in the Canadian Rocky Mountains. *Hydrology and Earth System Sciences*, 14(7), 1401–1415. <https://doi.org/10.5194/hess-14-1401-2010>
- Marks, D., Domingo, J., Susong, D., Link, T., & Garen, D. (1999). A spatially distributed energy balance snowmelt model for application in mountain basins. *Hydrological Processes*, 13(12-13), 1935–1959. [https://doi.org/10.1002/\(sici\)1099-1085\(199909\)13:12/13<1935::aid-hyp868>3.0.co;2-c](https://doi.org/10.1002/(sici)1099-1085(199909)13:12/13<1935::aid-hyp868>3.0.co;2-c)
- Martinez, G. F., & Gupta, H. V. (2010). Toward improved identification of hydrological models: A diagnostic evaluation of the “abcd” monthly water balance model for the conterminous United States. *Water Resources Research*, 46(8).
- Mazurkiewicz, A. B., Callery, D. G., & McDonnell, J. J. (2008). Assessing the controls of the snow energy balance and water available for runoff in a rain-on-snow environment. *Journal of Hydrology*, 354(1–4), 1–14.
- McCabe, G. J., & Markstrom, S. L. (2007). *A Monthly Water-Balance Model Driven by a Graphical User Interface* (Vol. 1088). US Geological Survey.
- Miller, D. M. (1982). *Water at the surface of Earth: An introduction to ecosystem hydrodynamics* (Vol. 21). Academic Press.
- Milly, P. C. D. (1994). Climate, soil water storage, and the average annual water balance. *Water Resources Research*, 30(7), 2143–2156. <https://doi.org/10.1029/94wr00586>
- Moriassi, D. N., Arnold, J. G., Van Liew, M. W., Bingner, R. L., Harmel, R. D., & Veith, T. L. (2007). Model evaluation guidelines for systematic quantification of accuracy in watershed simulations. *Transactions of the ASABE*, 50(3), 885–900. <https://doi.org/10.13031/2013.23153>
- Mouelhi, S., Michel, C., Perrin, C., & Andréassian, V. (2006). Stepwise development of a two-parameter monthly water balance model. *Journal of Hydrology*, 318(1–4), 200–214.
- Nash, J. E., & Sutcliffe, J. V. (1970). River flow forecasting through conceptual models part I—a discussion of principles. *Journal of Hydrology*, 10(3), 282–290. [https://doi.org/10.1016/0022-1694\(70\)90255-6](https://doi.org/10.1016/0022-1694(70)90255-6)
- Orth, R., Staudinger, M., Seneviratne, S. I., Seibert, J., & Zappa, M. (2015). Does model performance improve with complexity? A case study with three hydrological models. *Journal of Hydrology*, 523, 147–159. <https://doi.org/10.1016/j.jhydrol.2015.01.044>
- Oudin, L., Hervieu, F., Michel, C., Perrin, C., Andréassian, V., Anctil, F., & Loumagne, C. (2005). Which potential evapotranspiration input for a lumped rainfall–runoff model? Part 2—towards a simple and efficient potential evapotranspiration model for rainfall–runoff modelling. *Journal of Hydrology*, 303(1–4), 290–306. <https://doi.org/10.1016/j.jhydrol.2004.08.026>
- Padrón, R. S., Gudmundsson, L., Greve, P., & Seneviratne, S. I. (2017). Large-scale controls of the surface water balance over land: Insights from a systematic review and meta-analysis. *Water Resources Research*, 53(11), 9659–9678
- Peel, M. C., Chiew, F. H., Western, A. W., & McMahon, T. A. (2000). Extension of unimpaired monthly streamflow data and regionalisation of parameter values to estimate streamflow in ungauged catchments. *Report to the National Land and Water Resources Audit*.
- Petersen, T., Devineni, N., & Sankarasubramanian, A. (2012). Seasonality of monthly runoff over the continental United States: Causality and relations to mean annual and mean monthly distributions of moisture and energy. *Journal of Hydrology*, 468, 139–150. <https://doi.org/10.1016/j.jhydrol.2012.08.028>
- Petersen, T., Devineni, N., & Sankarasubramanian, A. (2018). Monthly hydroclimatology of the continental United States. *Advances in Water Resources*, 114, 180–195. <https://doi.org/10.1016/j.advwatres.2018.02.010>
- Pierson, D. C., Samal, N. R., Owens, E. M., Schneiderman, E. M., & Zion, M. S. (2013). Changes in the timing of snowmelt and the seasonality of nutrient loading: Can models simulate the impacts on freshwater trophic status? *Hydrological Processes*, 27(21), 3083–3093. <https://doi.org/10.1002/hyp.9894>
- Pike, J. G. (1964). The estimation of annual run-off from meteorological data in a tropical climate. *Journal of Hydrology*, 2(2), 116–123. [https://doi.org/10.1016/0022-1694\(64\)90022-8](https://doi.org/10.1016/0022-1694(64)90022-8)
- Rantz, S. E. (1982). *Measurement and Computation of Streamflow* (Vol. 2175). US Department of the Interior, Geological Survey.
- Reba, M. L., Pomeroy, J., Marks, D., & Link, T. E. (2012). Estimating surface sublimation losses from snowpacks in a mountain catchment using eddy covariance and turbulent transfer calculations. *Hydrological Processes*, 26(24), 3699–3711. <https://doi.org/10.1002/hyp.8372>
- Reggiani, P., Sivapalan, M., & Hassanizadeh, S. M. (2000). Conservation equations governing hillslope responses: Exploring the physical basis of water balance. *Water Resources Research*, 36(7), 1845–1863. <https://doi.org/10.1029/2000wr900066>
- Sankarasubramanian, A., & Vogel, R. M. (2002). Annual hydroclimatology of the United States. *Water Resources Research*, 38(6), 19–21. <https://doi.org/10.1029/2001wr000619>
- Sankarasubramanian, A., Wang, D., Archfield, S., Reitz, M., Vogel, R. M., Mazrooei, A., & Mukhopadhyay, S. (2020). HESS Opinions: Beyond the long-term water balance: Evolving Budyko's supply–demand framework for the Anthropocene towards a global synthesis of land-surface fluxes under natural and human-altered watersheds. *Hydrology and Earth System Sciences*, 24(4), 1975–1984
- Schaeffli, B., & Gupta, H. V. (2007). Do Nash values have value? *Hydrological Processes: International Journal*, 21(15), 2075–2080. <https://doi.org/10.1002/hyp.6825>
- Schreiber, P. (1904). Über die Beziehungen zwischen dem Niederschlag und der Wasserführung der Flüsse in Mitteleuropa. *Zeitschrift für Meteorologie*, 21(10), 441–452.
- Shook, K., & Gray, D. M. (1997). Snowmelt resulting from advection. *Hydrological Processes*, 11(13), 1725–1736. [https://doi.org/10.1002/\(sici\)1099-1085\(19971030\)11:13<1725::aid-hyp601>3.0.co;2-p](https://doi.org/10.1002/(sici)1099-1085(19971030)11:13<1725::aid-hyp601>3.0.co;2-p)
- Sivapalan, M., Takeuchi, K., Franks, S. W., Gupta, V. K., Karambiri, H., Lakshmi, V., & Zehe, E. (2003). IAHS decade on predictions in ungauged basins (PUB), 2003–2012: Shaping an exciting future for the hydrological sciences. *Hydrological Sciences Journal*, 48(6), 857–880. <https://doi.org/10.1623/hysj.48.6.857.51421>
- Sivapalan, M., & Young, P. C. (2006). *Downward approach to hydrological model development*. Encyclopedia of hydrological sciences.

- Slack, J. R., Lumb, A., & Landwehr, J. M. (1993). *Hydro-climatic data network (HCDN) streamflow data set, 1874-1998. CD-ROM*. US Geological Survey. Retrieved from <http://www.daac.ornl.gov>
- Sposito, G. (2017). Understanding the Budyko equation. *Water*, 9(4), 236.
- Stewart, I. T., Cayan, D. R., & Dettinger, M. D. (2005). Changes toward earlier streamflow timing across western North America. *Journal of climate*, 18(8), 1136–1155.
- Strasser, U., Bernhardt, M., Weber, M., Liston, G. E., & Mauser, W. (2008). Is snow sublimation important in the alpine water balance? *The Cryosphere*, 2(1), 53–66. <https://doi.org/10.5194/tc-2-53-2008>
- Tekleab, S., Uhlenbrook, S., Mohamed, Y., Savenije, H. H. G., Temesgen, M., & Wenninger, J. (2011). Water balance modeling of Upper Blue Nile catchments using a top-down approach. *Hydrology and Earth System Sciences*, 15(7), 2179–2193. <https://doi.org/10.5194/hess-15-2179-2011>
- TheMathworksInc. (2016). *Optimization toolbox: User's guide*. Retrieved from [https://www.mathworks.com/help/pdf\\_doc/gads/gads](https://www.mathworks.com/help/pdf_doc/gads/gads)
- Thomas, H. A. (1981). *Improved methods for national water assessment*. Report WR15249270. US Water Resource Council.
- Thornthwaite, C. W. (1948). An approach toward a rational classification of climate. *Geographical Review*, 38(1), 55–94. <https://doi.org/10.2307/210739>
- Vandewiele, G. L., & Ni-Lar-Win (1998). Monthly water balance models for 55 basins in 10 countries. *Hydrological Sciences Journal*, 43(5), 687–699. <https://doi.org/10.1080/02626669809492166>
- Vandewiele, G. L., & Xu, C. Y. (1992). Methodology and comparative study of monthly water balance models in Belgium, China and Burma. *Journal of Hydrology*, 134(1-4), 315–347.
- Vanlier, J., Tiemann, C. A., Hilbers, P. A., & van Riel, N. A. (2014). Optimal experiment design for model selection in biochemical networks. *BMC Systems Biology*, 8(1), 1–16. <https://doi.org/10.1186/1752-0509-8-20>
- Viviroli, D., Archer, D. R., Buytaert, W., Fowler, H. J., Greenwood, G. B., Hamlet, A. F., & Woods, R. (2011). Climate change and mountain water resources: Overview and recommendations for research, management and policy. *Hydrology and Earth System Sciences*, 15(2), 471–504. <https://doi.org/10.5194/hess-15-471-2011>
- Vogel, R. M., & Sankarasubramanian, A. (2005). *USGS hydro-climatic data network (HCDN): Monthly climate database, 1951–1990*. Data set available on-line from Oak Ridge National Laboratory Distributed Active Archive Center. <https://doi.org/10.3334/ORNLDAAC/810>
- Vogel, R. M., Wilson, L., & Daly, C. (1999). Regional regression models of annual streamflow for the United States. *Journal of Irrigation and Drainage Engineering*, 125(3), 148–157. [https://doi.org/10.1061/\(asce\)0733-9437\(1999\)125:3\(148\)](https://doi.org/10.1061/(asce)0733-9437(1999)125:3(148))
- Wang, C., Wang, S., Fu, B., & Zhang, L. (2016). Advances in hydrological modelling with the Budyko framework: A review. *Progress in Physical Geography*, 40(3), 409–430.
- Wang, D., & Tang, Y. (2014). A one-parameter Budyko model for water balance captures emergent behavior in Darwinian hydrologic models. *Geophysical Research Letters*, 41(13), 4569–4577. <https://doi.org/10.1002/2014gl060509>
- Wang, G. Q., Zhang, J. Y., Jin, J. L., Liu, Y. L., He, R. M., Bao, Z. X., et al. (2014). Regional calibration of a water balance model for estimating stream flow in ungauged areas of the Yellow River Basin. *Quaternary International*, 336, 65–72.
- Wang, Q. J., Pagano, T. C., Zhou, S. L., Hapuarachchi, H. A. P., Zhang, L., & Robertson, D. E. (2011). Monthly versus daily water balance models in simulating monthly runoff. *Journal of Hydrology*, 404(3–4), 166–175. <https://doi.org/10.1016/j.jhydrol.2011.04.027>
- Wu, C., Yeh, P. J. F., Hu, B. X., & Huang, G. (2018). Controlling factors of errors in the predicted annual and monthly evaporation from the Budyko framework. *Advances in Water Resources*, 121, 432–445. <https://doi.org/10.1016/j.advwatres.2018.09.013>
- Wu, H., Adler, R. F., Tian, Y., Huffman, G. J., Li, H., & Wang, J. (2014). Real-time global flood estimation using satellite-based precipitation and a coupled land surface and routing model. *Water Resources Research*, 50(3), 2693–2717. <https://doi.org/10.1002/2013wr014710>
- Xiong, L., & Guo, S. (1999). A two-parameter monthly water balance model and its application. *Journal of hydrology*, 216(1-2), 111–123.
- Xu, C. Y., & Singh, V. P. (1998). A review on monthly water balance models for water resources investigations. *Water Resources Management*, 12(1), 20–50. <https://doi.org/10.1023/a:1007916816469>
- Yang, D., Sun, F., Liu, Z., Cong, Z., Ni, G., & Lei, Z. (2007). Analyzing spatial and temporal variability of annual water-energy balance in non-humid regions of China using the Budyko hypothesis. *Water Resources Research*, 43(4). <https://doi.org/10.1029/2006wr005224>
- Zhang, D., Cong, Z., Ni, G., Yang, D., & Hu, S. (2015). Effects of snow ratio on annual runoff within the Budyko framework. *Hydrology and Earth System Sciences*, 19(4), 1977–1992. <https://doi.org/10.5194/hess-19-1977-2015>
- Zhang, L., Dawes, W. R., & Walker, G. R. (2001). Response of mean annual evapotranspiration to vegetation changes at catchment scale. *Water Resources Research*, 37(3), 701–708. <https://doi.org/10.1029/2000wr900325>
- Zhang, L., Hickel, K., Dawes, W. R., Chiew, F. H., Western, A. W., & Briggs, P. R. (2004). A rational function approach for estimating mean annual evapotranspiration. *Water Resources Research*, 40(2). <https://doi.org/10.1029/2003wr002710>
- Zhang, L., Potter, N., Hickel, K., Zhang, Y., & Shao, Q. (2008). Water balance modeling over variable time scales based on the Budyko framework—Model development and testing. *Journal of Hydrology*, 360(1–4), 117–131. <https://doi.org/10.1016/j.jhydrol.2008.07.021>
- Zhang, T., Barry, R. G., Knowles, K., Ling, F., & Armstrong, R. L. (2003). Distribution of seasonally and perennially frozen ground in the Northern Hemisphere. *Proceedings of the 8th International Conference on Permafrost, Zürich, Switzerland* (Vol. 2, pp. 1289–1294). AA Balkema Publishers.
- Zhou, G., Wei, X., Chen, X., Zhou, P., Liu, X., Xiao, Y., & Su, Y. (2015). Global pattern for the effect of climate and land cover on water yield. *Nature Communications*, 6(1), 1–9. <https://doi.org/10.1038/ncomms6918>